© 2015. Published by The Company of Biologists Ltd | Development (2015) 142, 3009-3020 doi:10.1242/dev.122176

RESEARCH ARTICLE

Meis1 coordinates a network of genes implicated in eye development and microphthalmia

Séverine Marcos[1,2], Monica González-Lázaro[3], Leonardo Beccari[1,2], Laura Carramolino[3], Maria Jesus Martin-Bermejo[1,2], Oana Amarie[4], Daniel Mateos-San Martín[3], Carlos Torroja[5], Ozren Bogdanović[6,7], Roisin Doohan[3], Oliver Puk[4], Martin Hrabě de Angelis[4], Jochen Graw[4], Jose Luis Gomez-Skarmeta[6], Fernando Casares[6], Miguel Torres[3,*] and Paola Bovolenta[1,2,*]

ABSTRACT

Microphthalmos is a rare congenital anomaly characterized by reduced eye size and visual deficits of variable degree. Sporadic and hereditary microphthalmos have been associated with heterozygous mutations in genes fundamental for eye development. Yet, many cases are idiopathic or await the identification of molecular causes. Here we show that haploinsufficiency of *Meis1*, which encodes a transcription factor with evolutionarily conserved expression in the embryonic trunk, brain and sensory organs, including the eye, causes microphthalmic traits and visual impairment in adult mice. By combining analysis of *Meis1* loss-of-function and conditional *Meis1* functional rescue with ChIP-seq and RNA-seq approaches we show that, in contrast to its preferential association with Hox-Pbx BSs in the trunk, Meis1 binds to Hox/Pbx-independent sites during optic cup development. In the eye primordium, Meis1 coordinates, in a dose-dependent manner, retinal proliferation and differentiation by regulating genes responsible for human microphthalmia and components of the Notch signaling pathway. In addition, Meis1 is required for eye patterning by controlling a set of eye territory-specific transcription factors, so that in *Meis1*$^{-/-}$ embryos boundaries among the different eye territories are shifted or blurred. We propose that *Meis1* is at the core of a genetic network implicated in eye patterning/microphthalmia, and represents an additional candidate for syndromic cases of these ocular malformations.

KEY WORDS: Developmental disorders, Notch signaling, Patterning, TALE transcription factors, Microphthalmia, Mouse

INTRODUCTION

Eye formation initiates with the specification of the retinal field in the anterior neural plate followed by morphogenetic rearrangement of retinal progenitors to form the optic vesicles. Subsequent interaction of the optic neuroepithelium with the surrounding tissue generates the optic cup, which is concomitantly patterned along its three main axes: proximodistal, nasotemporal and dorsoventral. This results in the formation of the neural retina, retinal pigment epithelium (RPE), optic stalk and lens (Martinez-Morales et al., 2004), the proliferation and differentiation of which generate a mature eye (Esteve and Bovolenta, 2006). Disruption of any of these events leads to ocular malformations, including anophthalmia (complete absence of the ocular globe) or microphthalmia (significant reduction of the globe axial length), which, in turn, cause severe visual deficits that, for microphthalmia, account for up to 11% of infant blindness in developed countries (Bardakjian and Schneider, 2011).

Cases of anophthalmia and microphthalmia have been associated with homozygous and heterozygous mutations in genes at the core of forebrain regulatory networks (Beccari et al., 2013), such as the transcription factors (TFs) *SOX2* (Fantes et al., 2003), *OTX2* (Ragge et al., 2005), *PAX6* (Glaser et al., 1994), *VSX2* (*CHX10*) (Ferda Percin et al., 2000), *RAX* (Voronina et al., 2004), *FOXE3* (Reis et al., 2010) and perhaps *SIX6* (Gallardo et al., 2004); in key components of cell to cell communication, including *SHH* (Schimmenti et al., 2003) and *BMP4* (Reis et al., 2011); or in genes involved in retinal progenitor proliferation and survival such as *STRA6* (Pasutto et al., 2007; White et al., 2008), *BCOR* (Ng et al., 2004), *HCCS* (Indrieri et al., 2013; Morleo et al., 2005) and *SMOC1* (Abouzeid et al., 2011; Okada et al., 2011). Yet, only a minor proportion of patients receive an accurate molecular diagnosis of the pathogenesis of their ocular malformation (Bardakjian and Schneider, 2011; Williamson and FitzPatrick, 2014), indicating that additional causative genes need to be identified. Given that anophthalmia and microphthalmia frequently occur in association with other birth defects, most commonly involving anomalies of the limbs, face, ears and skeletal muscle system (Slavotinek, 2011), genes implicated in multiple aspects of embryonic development, such as *Meis1*, are good candidates to be explored.

Meis1, its *Drosophila* homolog *homothorax* (*hth*) and the related *Meis2* and *Meis3*, belong to a subfamily of TALE (three amino acid loop extension) homeodomain-containing TFs (Longobardi et al., 2014). Meis proteins form stable heteromeric complexes with other transcriptional regulators, enhancing their affinity and specificity of binding to DNA sites in the target gene locus (Penkov et al., 2013; Slattery et al., 2011). For example, together with Pbx1, Meis1 plays a major role as a co-factor for the TFs of the Hox complex, which, in turn, have a pivotal and evolutionarily conserved role in orchestrating embryonic trunk development (Duboule, 2007; Mallo and Alonso, 2013). In accordance with this notion, loss of *Meis1* function impairs the formation of *Meis1*-expressing trunk organs and systems, such as the limbs, heart, blood and vasculature (Azcoitia et al., 2005; Erickson et al., 2010; Hisa et al., 2004; Mercader et al., 1999, 2009; Zhang et al., 2002).

Members of the Meis subfamily are however also expressed in the brain and sensory organs (Schulte and Frank, 2014), which are Hox-

[1]Centro de Biología Molecular "Severo Ochoa", CSIC-UAM, c/Nicolás Cabrera, 1, Madrid E-28049, Spain. [2]CIBER de Enfermedades Raras (CIBERER), c/Nicolás Cabrera, 1, Madrid E-28049, Spain. [3]Departamento de Desarrollo y Reparación Cardiovascular, Centro Nacional de Investigaciones Cardiovasculares (CNIC), c/Melchor Fernández Almagro, 3, Madrid E-28029, Spain. [4]Institute of Developmental Genetics Helmholtz Center Munich, Neuherberg D-85764, Germany. [5]Bioinformatics Unit, Centro Nacional de Investigaciones Cardiovasculares (CNIC), c/Melchor Fernández Almagro, 3, Madrid E-28029, Spain. [6]Centro Andaluz de Biología del Desarrollo (CABD), CSIC-UPO, Carretera de Utrera Km1, Sevilla E-41013, Spain. [7]ARC Center of Excellence in Plant Energy Biology, School of Chemistry and Biochemistry, Faculty of Science, The University of Western Australia, Perth, Western Australia 6009, Australia.

*Authors for correspondence (mtorres@cnic.es; pbovolenta@cbm.csic.es)

Received 15 January 2015; Accepted 17 July 2015

Development (2015) 142, 3009-3020 doi:10.1242/dev.122176

free embryonic regions (Duboule, 2007; Mallo and Alonso, 2013). In particular, *Meis1* is expressed in the vertebrate forebrain and sensory organ primordia, including the eye, being essential for the specification of part of these structures. Indeed, genetic inactivation of *Meis1* in mice causes lens reduction and abnormal retinal morphology (Hisa et al., 2004). Cardiovascular-related embryonic lethality of *Meis1*$^{-/-}$ embryos (Azcoitia et al., 2005; Hisa et al., 2004) and the virtual lack of information on the alternative and Hox-independent transcriptional mechanisms that Meis1 must adopt in the head region (Longobardi et al., 2014) have presented hurdles to understanding why and how these eye defects arise.

Here, we have begun to address these issues by taking advantage of *Meis1* loss-of-function and conditional *Meis1* functional rescue in mice, combined with ChIP-seq and RNA-seq approaches. Our results indicate that Meis1, by binding to 'Meis-only' binding sites in the DNA, regulates (directly and indirectly) the expression of genes involved in patterning, proliferation and differentiation of the neural retina, including components of the Notch signaling pathway. Meis1 is also at the core of a genetic network implicated in mammalian microphthalmia, and its haploinsufficiency suffices to cause microphthalmic traits in adult mice, suggesting that *Meis1* itself represents an additional candidate for this ocular malformation.

RESULTS

Meis1 deficiency causes embryonic microphthalmia

Meis1 is uniformly expressed in the zebrafish and chick eye primordium and progressively retracts from the central retina following the wave of retinal cell differentiation (Bessa et al., 2008; Heine et al., 2008). In both species, *Meis1* regulates the expression of cyclin D1 (*Ccnd1*), thereby promoting G1-S transition of retinal cells and thus the generation of sufficient numbers of retinal progenitors (Bessa et al., 2008; Heine et al., 2008). Accordingly, interference with *Meis1* expression causes eye hypoplasia (Bessa et al., 2008; Heine et al., 2008).

We reproduced these observations in mice. *Meis1* mRNA localized to the eye field (Fig. 1). Its expression (Fig. 1A-E) and that of its protein (Fig. 1I-K) was thereafter maintained in the optic neuroepithelium and the overlying surface ectoderm throughout eye formation, according to the distribution detected with a *lacZ* reporter (Hisa et al., 2004). Meis1 expression was also maintained in retinal neurons as defined by its co-expression with the neuronal differentiation marker Tuj1 (Tubb3) (Fig. 1L,M). Although *Meis2* has been reported to be transiently expressed in E9.5 optic vesicles (Heine et al., 2008), we could not detect *Meis2* expression at any early stages of eye development (Fig. 1F-H). Thus, early mouse eye development seems to depend mostly on *Meis1* function, in contrast to what has been observed in zebrafish and chick, where *Meis2* is instead clearly detected (Bessa et al., 2008; Heine et al., 2008).

Complete inactivation of *Meis1* caused lens vesicle reduction, as described using a different *Meis1*$^{-/-}$ mouse line (Hisa et al., 2004), but we did not observe the reported retinal duplication (Hisa et al., 2004). Instead, we noticed a significant reduction of the optic cup compared with wild-type (wt) littermates. This reduction was first apparent at E11 (Fig. 2) and became accentuated with development, especially in the ventral side, so that E13 *Meis1*$^{-/-}$ eyes were roughly half the size of those of wt (Fig. 2S). This was associated with a significant decrease in BrdU incorporation and *Ccnd1* expression (Fig. 2A-C,T; supplementary material Fig. S1D-F), although there was no statistically significant difference in the mitotic index [calculated as the number of cells in M phase (phospho-histone H3^{+})/area] among wt and *Meis1* null embryos in both the neural retina and the RPE (Fig. 2U).

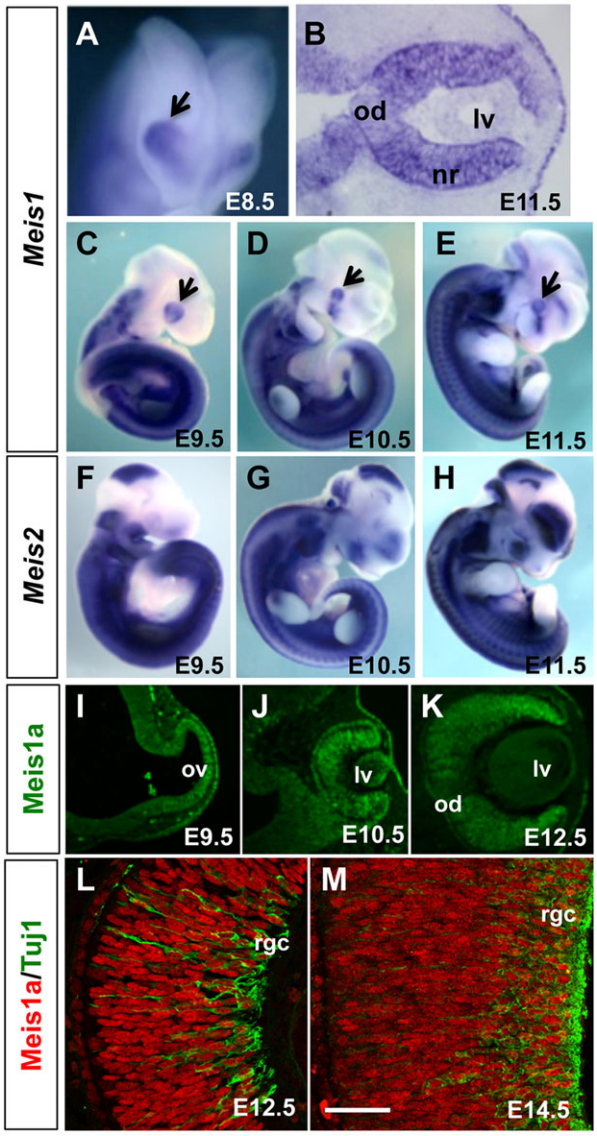

Fig. 1. Embryonic expression of *Meis1* and *Meis2*. (A-H) Frontal (A) and lateral (C-H) views of mouse embryos at stages between E8.5 and E11.5 hybridized *in toto* with probes specific for *Meis1* and *Meis2*. (B) Frontal paraffin section through the optic cup of an E11.5 mouse embryo hybridized with a probe against *Meis1*. Note that *Meis1* is strongly expressed in the eye field (arrow in A) and its expression is maintained as the optic cup forms (arrows in C-E). The expression is particularly abundant in the neural retina (B). *Meis2* is not expressed in the developing eye (F-H) but is strongly expressed in the mesencephalon and spinal cord. (I-M) Frontal cryostat sections of mouse embryos at stages between E9.5 and E14.5 were immunostained with antibodies against Meis1a, (one of the Meis1 isoforms) or co-immunostained with the neuronal differentiation marker Tuj1 (L,M). Note that Meis1a is detected in the entire optic vesicle and overlying ectoderm, in the developing optic cup and in differentiated neurons. lv, lens vesicle; nr, neural retina; od, optic disc; ov, optic vesicle; rgc, retinal ganglion cells. Scale bar: 25 µm.

Together, these observations indicate that the proposed Hth/Meis1-mediated control of retinal progenitor proliferation is conserved in mice and complete loss of *Meis1* function drastically affects ocular development, causing microphthalmia.

Microphthalmia is associated with decreased neurogenesis and increased apoptosis

Previous studies in *Drosophila* and zebrafish retina have shown that Meis1/Hth expression is turned off in differentiating cells and its

Development (2015) 142, 3009-3020 doi:10.1242/dev.122176

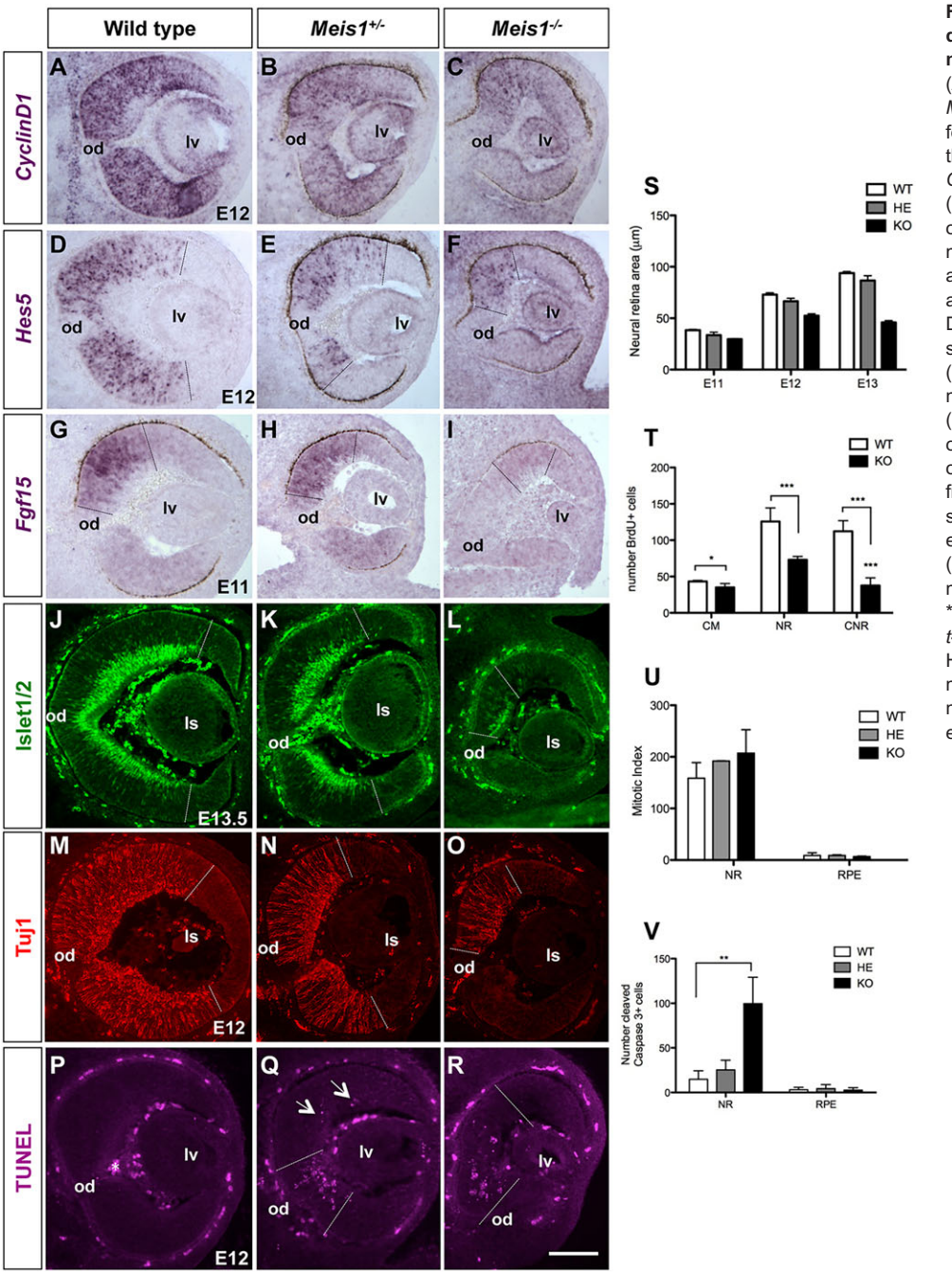

Fig. 2. *Meis1* loss of function causes dose-dependent alterations in retinal neurogenesis leading to microphthalmia. (A-R) Frontal sections of E11-E13.5 wt, *Meis1*$^{+/-}$ and *Meis1*$^{-/-}$ optic cups processed for the indicated markers. Compared with the wt, note the decreased proliferation (less *Ccnd1* expression) and the impaired onset (*Fgf15*, *Hes5*) and progression (Isl1/2, Tuj1) of neuronal differentiation in the *Meis1* mutants, associated with increased apoptosis (P-R). Absence of one *Meis1* allele suffices to induce these defects. Dotted lines delineate the extent of marker staining. Arrows (Q) indicate apoptotic cells. (S-V) Quantification of neural retina area (S), number of BrdU^{+} cells (T), mitotic index (phospho-histone H3^{+}/area, U) and number of cleaved caspase 3^{+} cells (V) in E12.5 optic cups. Total areas were determined from DAPI-stained sections. Error bars are s.e.m. of counting all sections from both eyes of at least three different embryos (n=3). There is no statistical difference in the mitotic index of the different genotypes (U). *P<0.05, **P<0.01, ***P<0.001 (Student's t-test). ls, lens; lv, lens vesicle; od, optic disc; HE, *Meis1*$^{+/-}$; KO, *Meis1*$^{-/-}$; CM, ciliary margin; CNR, central neural retina; NR, neural retina; RPE, retinal pigmented epithelium. Scale bar: 25 µm.

forced maintenance prevents the acquisition of a differentiated neuronal fate (Bessa et al., 2002, 2008). This downregulation was not observed in the embryonic mouse retina, in which differentiated neurons are still Meis1 positive (Fig. 1M). We thus examined whether the reduced eye size of *Meis1* null mouse embryos is also associated with abnormal neurogenesis.

We first compared the onset of Fgf signaling, which triggers retinal neurogenesis (Martinez-Morales et al., 2005), in E11.5 wt and mutant embryos. *Fgf15* was strongly expressed in the wt central retina but was visibly reduced in both level and extent in *Meis1*$^{-/-}$ embryos (Fig. 2G-I). Furthermore, the number of Otx2^{+} retinal progenitors (supplementary material Fig. S1G,I) (Bovolenta et al., 1997) and that of Tuj1^{+} or islet 1/2 (Isl1/2)$^{+}$ differentiating neurons (Esteve et al., 2011) was reduced in E12/E13 *Meis1*$^{-/-}$ retinas (Fig. 2J,L,M,O). In contrast to what has been reported in zebrafish and chick (Bessa et al., 2008; Heine et al., 2008), in *Meis1* null embryos, but not in wt, the prospective neural retina at E12.5-E13.5 showed a significant number of TUNEL^{+} and cleaved caspase 3^{+} apoptotic cells (Fig. 2P-R,V). The majority of apoptotic cells were concentrated in the regions of ongoing neuronal differentiation (compare Fig. 2O with 2R), suggesting a link between the two events.

Haploinsufficiency of *Meis1* causes microphthalmic traits in adult mice

In humans, microphthalmia is often caused by dominant heterozygous mutations, especially when mutations hit genes fundamental for eye development (Williamson and FitzPatrick, 2014). We thus investigated if loss of one *Meis1* allele suffices to impair eye growth. Indeed, the size of the eye in *Meis*$^{+/-}$ embryos

Development (2015) 142, 3009-3020 doi:10.1242/dev.122176

was slightly reduced in all of the embryos analyzed (30/30) as compared with wt (Fig. 2A,B,D,E,G,H,S) and associated with an evident decrease in *Ccnd1* expression (Fig. 2B). Furthermore, the domain of expression of markers implicated in neuronal differentiation, including *Fgf15*, *Otx2*, Isl1/2 and Tuj1, was smaller than that observed in wt littermates but not as reduced as that in *Meis1*$^{-/-}$ embryos (Fig. 2G-O; supplementary material Fig. S1G-I). As in homozygous mutants, the retinas of *Meis1*$^{+/-}$ embryos presented an increased number of apoptotic cells in the region of active neurogenesis (Fig. 2Q).

Altogether, these observations suggested that heterozygous embryos present a milder version of the ocular phenotype seen in *Meis1* null mice. To confirm this and exclude the possibility that reduced *Meis1* function might simply delay eye development, we examined whether the observed embryonic defects persisted into adulthood, as *Meis*$^{+/-}$ mice, in contrast to homozygous mice, are viable and fertile.

Scheimpflug imaging revealed no anterior segment abnormality in adult *Meis*$^{+/-}$ animals as compared with wt littermates (supplementary material Fig. S2). Likewise, optical coherence tomography (OCT) showed no defects in the number and distribution of the main blood vessels when adult wt and *Meis1* heterozygous animals were compared (Fig. 3A,B). By contrast, non-invasive analysis of left and right eye morphometrics and histological analysis of the retina showed that in *Meis1*$^{+/-}$ mice the axial length of the optic globe and the thickness of the neural retina were significantly decreased (Fig. 3C-H). This reduced thickness seemed to affect, albeit slightly, all nuclear layers (Fig. 3E,F) and could result from the decrease in neurogenesis observed in the heterozygous embryos coupled to the increase in apoptosis. Notably, these morphological changes were associated with a significant loss of visual performance (Fig. 3I), as determined by the virtual drum vision test (Prusky et al., 2004).

Thus, haploinsufficiency of *Meis1* causes morphological and functional defects characteristic of microphthalmia (Williamson and FitzPatrick, 2014). Microphthalmia is likely to be a direct consequence of Meis1 requirement in the retinal neuroepithelium since blood vessels and lens, which may both influence retinal development, formed normally.

Microphthalmia is not a consequence of *Meis1* function in the vascular system

To further confirm the idea that the microphthalmia observed in *Meis1* mutant embryos is independent from the abnormal development of the hematopoietic/vascular system characteristic of *Meis1* null embryos (Azcoitia et al., 2005; Hisa et al., 2004), we analyzed a mouse line with a targeted rescue of Meis1 function in the hematopoietic and vascular system in a *Meis1a*$^{-/-}$ background [*Meis1a*$^{-/-}$*;Tie2Cre;R26Meis2a* (Rosello-Diez et al., 2014)].

In contrast to the evident rescue of the hemorrhage that is usually present in *Meis1* null embryos (Fig. 4A-C) (Rosello-Diez et al., 2014), the eye size of all of the analyzed *Meis1a*$^{-/-}$*;Tie2Cre;R26Meis2a* embryos (13/13) was still reduced and comparable to that observed in *Meis1a*$^{-/-}$*;Tie2Cre* littermates (Fig. 4A-C). Indeed, at E13 the area of the neural retina of *Meis1a*$^{-/-}$*;Tie2Cre;R26Meis2a* and *Meis1a*$^{-/-}$*;Tie2Cre* embryos was on average 47%

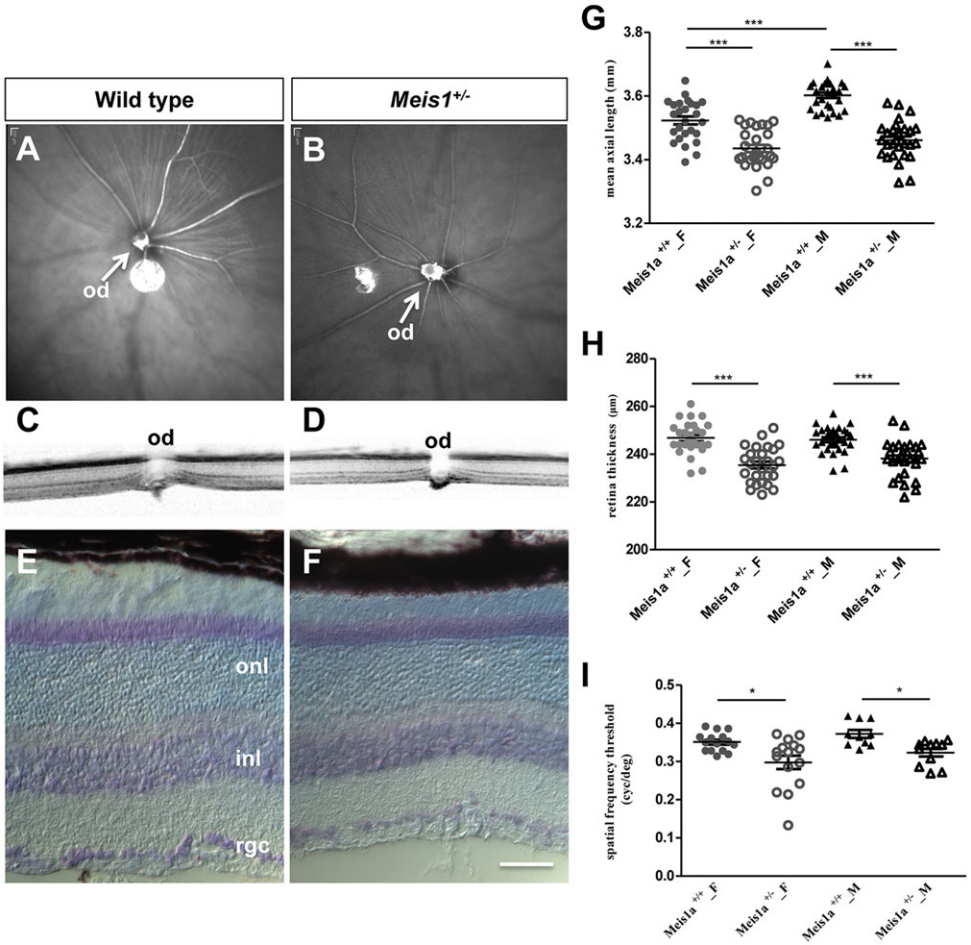

Fig. 3. Haploinsufficiency of *Meis1* causes microphthalmic traits in adult mice. (A,B) Retina fundus of wt and *Meis1*$^{+/-}$ adult eye obtained by OCT. No difference in the vasculature organization was detected between heterozygous (*n*=5) and wt (*n*=5) littermates. (C,D) Images of wt and *Meis1*$^{+/-}$ adult central retinas obtained by OCT. (E,F) Frontal cryostat sections of wt and *Meis1*$^{+/-}$ adult central retinas stained with Cresyl Violet. Note the slight difference in thickness of the various layers, leading to an overall reduced thickness of the retina in *Meis1*$^{+/-}$. (G) Eye size measurements by LIB revealed significantly reduced axial eye length in mutants of both sexes: females (F) and males (M). (H) Retinal thickness in both females and males was significantly decreased in *Meis1a*$^{+/-}$. (I) Virtual drum vision testing showed a reduced response in both female (*P*=0.012) and male (*P*=0.01) mutants. Error bars are s.e.m. of *n*=15 mice per group. **P*<0.05, ****P*<0.001 (Student's *t*-test). od, optic disc; onl, outer nuclear layer; inl, inner nuclear layer; rgc, retina ganglion cells. Scale bar: 25 µm.

Development (2015) 142, 3009-3020 doi:10.1242/dev.122176

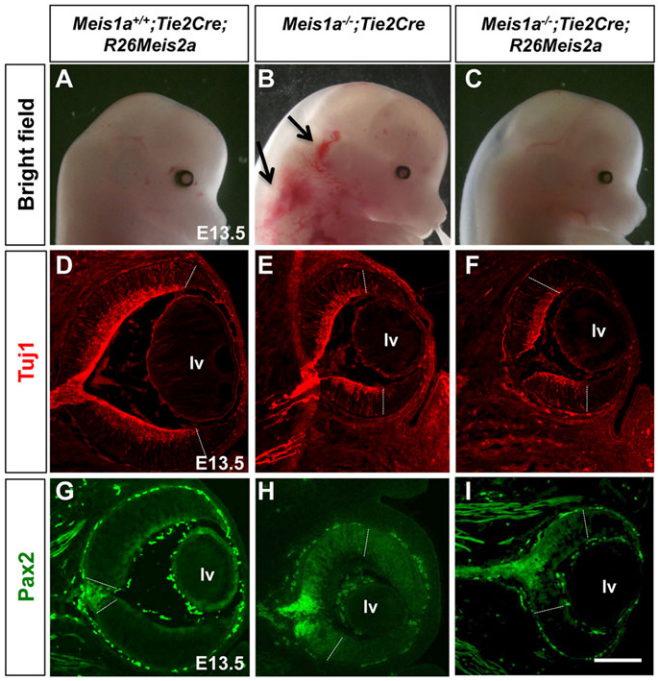

Fig. 4. Microphthalmia is not linked to *Meis1* function in the hematopoietic/vascular system. (A-C) Bright field lateral view of E13.5 *Meis1a*$^{+/+}$*;Tie2Cre;R26Meis2a*, *Meis1a*$^{-/-}$*;Tie2Cre* and *Meis1a*$^{-/-}$*;Tie2Cre; R26Meis2a* embryonic heads. Note that the hemorrhage evident in *Meis1a*$^{-/-}$ (arrows in B) is no longer observed in rescued embryos (C), although the eye size is still reduced (B,C) as compared with control littermates (A). (D-I) Frontal cryostat sections of the optic cup immunostained with antibodies against Tuj1 or Pax2. Note that the rescue of Meis1a expression in the vasculature does not improve neuronal differentiation and optic cup patterning defects. Dotted lines delineate the extent of marker labeling. lv, lens vesicle. Scale bar: 25 µm.

and 48.2% smaller, respectively, than that of the *Meis1a*$^{+/+}$*; Tie2Cre;R26Meis2a* control littermates. This reduction is very similar to that seen in *Meis1*$^{-/-}$ embryos (Fig. 2S).

Likewise, in both *Meis1a*$^{-/-}$*;Tie2Cre* and *Meis1a*$^{-/-}$*;Tie2Cre; R26Meis2a* E13.5 retinas, the number of Tuj1^{+} differentiating neurons was similarly reduced (Fig. 4D-F) and the expression of optic cup patterning markers altered. For example, and as observed in *Meis1* null embryos (supplementary material Fig. S1J-L; and see below), the distribution of the TF Pax2, which is normally restricted to cells of the optic disc at E12/E13 (Morcillo et al., 2006) (supplementary material Fig. S1J; Fig. 4G), was instead expanded in the ventral and dorsal retina of both *Meis1a*$^{-/-}$*;Tie2Cre* and *Meis1a*$^{-/-}$*;Tie2Cre;R26Meis2a* embryos (Fig. 4H,I), comparably to that observed in *Meis1* mutant embryos (supplementary material Fig. S1K,L).

Meis1 interacts with a set of enhancers specifically involved in eye development using Hox/Pbx-independent binding sites

Altogether, these data indicate that a full dose of *Meis1* is required for the progression of retina development. Reduced Meis1 levels prevent retinal progenitors from undertaking a normal proliferative and differentiation program, ultimately leading to the death of some cells. As previously noted (Heine et al., 2008), *Ccnd1* downregulation by itself is unlikely to explain this severe phenotype because retinal differentiation is normal in *Ccnd1*$^{-/-}$ mice (Sicinski et al., 1995) and overexpression of *Ccnd1* only partially rescues the effect of loss of *Meis1* function (Heine et al., 2008). Thus, besides *Ccnd1*, Meis1 is likely to regulate additional neurogenic pathways. This regulation must take place via a Hox/Pbx-independent mechanism because Hox genes, which are well-known partners of Meis in the trunk, are not expressed in the head (Schulte and Frank, 2014). Furthermore, there is no indication that Pbx genes contribute to early eye formation, even though compound knockout mice have been generated and extensively studied (Capellini et al., 2011; Stankunas et al., 2008).

To address this question and identify the binding sites (BSs) of endogenous Meis1 protein in the developing eye, we performed ChIP-seq analysis using isolated E10.5 optic cups, shortly before the detection of overt *Meis1*$^{-/-}$ eye defects. We identified a total of 5361 Meis1 BSs in the genome and a collection of 3182 genes with a transcription start site (TSS) closest to any Meis1 BS (GEO GSE62786). As previously reported (Penkov et al., 2013), most Meis1 BSs were located in regions remote from their closest associated TSS (Fig. 5A).

To study the functional relevance of Meis1 BSs we performed further ChIP-seq analysis of the E10.5 optic cup to determine histone modification marks that identify promoter (H3K4me3) and enhancer (H3K4me1) regions. Meis1 BSs associated very significantly with both H3K4me1 and H3K4me3 marks, indicating a preference for enhancer and promoter region binding (Fig. 5B). When comparing Meis preference for binding to H3K4me1 and H3K4me3 marks, as reported in other tissues (Penkov et al., 2013), we found that Meis1 preferentially binds to enhancer regions (Fig. 5B). Meis1 selects two main sequences in the embryonic trunk: the Pbx-Hox binding sequence (A/TGATNNAT), to which it binds indirectly, and a direct BS (TGACAG) (Penkov et al., 2013). To determine binding preferences in the developing eye, we identified consensus sequences in the E10.5 eye Meis BS collection. We found only one consensus sequence showing a unimodal distribution, with the maximum mapping to the center of the Meis BS and therefore representing the Meis1-bound core sequence (m1 sequence, Fig. 5C). We identified three additional consensus sequences showing a bimodal distribution, with maxima mapping at a certain distance from the Meis BS center, which are likely to represent cooperating sequences not directly bound by Meis1 (m2-m3, Fig. 5C). The m1 consensus is a very close variant of the Meis1 direct binding sequence identified in the trunk (Penkov et al., 2013), whereas m2-m3 sequences are low-complexity or rather relaxed sequences that we could not correlate to previously described consensus binding motifs.

These results suggest that in the eye Meis1 selects BSs and sequences unrelated to the Hox-Pbx network. In support of this view, the prominent pattern of Meis binding to the *HoxA* cluster seen in the trunk is completely absent in the E10.5 eye (Fig. 5D). We then looked for previously described Meis-regulated enhancers in the developing eye. Within the Meis1 BS collection, we found the previously described Meis BS in the *Pax6* lens ectoderm enhancer (Zhang et al., 2002) and an additional peak in the *Pax6* third intron, but not the *Pax6*-associated Meis BS reported after embryonic trunk ChIP-seq (Penkov et al., 2013) or those found in a pancreatic enhancer (Zhang et al., 2006) (Fig. 5E). The eye-specific Meis1 BS coincided with H3K4me1^{high}/H3K4me3^{low} marks typical of enhancer regions (Fig. 5E).

Remarkably, despite the distance between Meis1 BSs and TSSs, the analysis of 'biological process' and 'MGI phenotypes' Gene Ontology (GO) classes for the Meis1 BS-associated genes identified eye development classes as the most overrepresented, with a predominance of 'eye size' and 'eye morphology' categories (Fig. 5F). Thus, the Meis1 binding profile reveals its functional

Development (2015) 142, 3009-3020 doi:10.1242/dev.122176

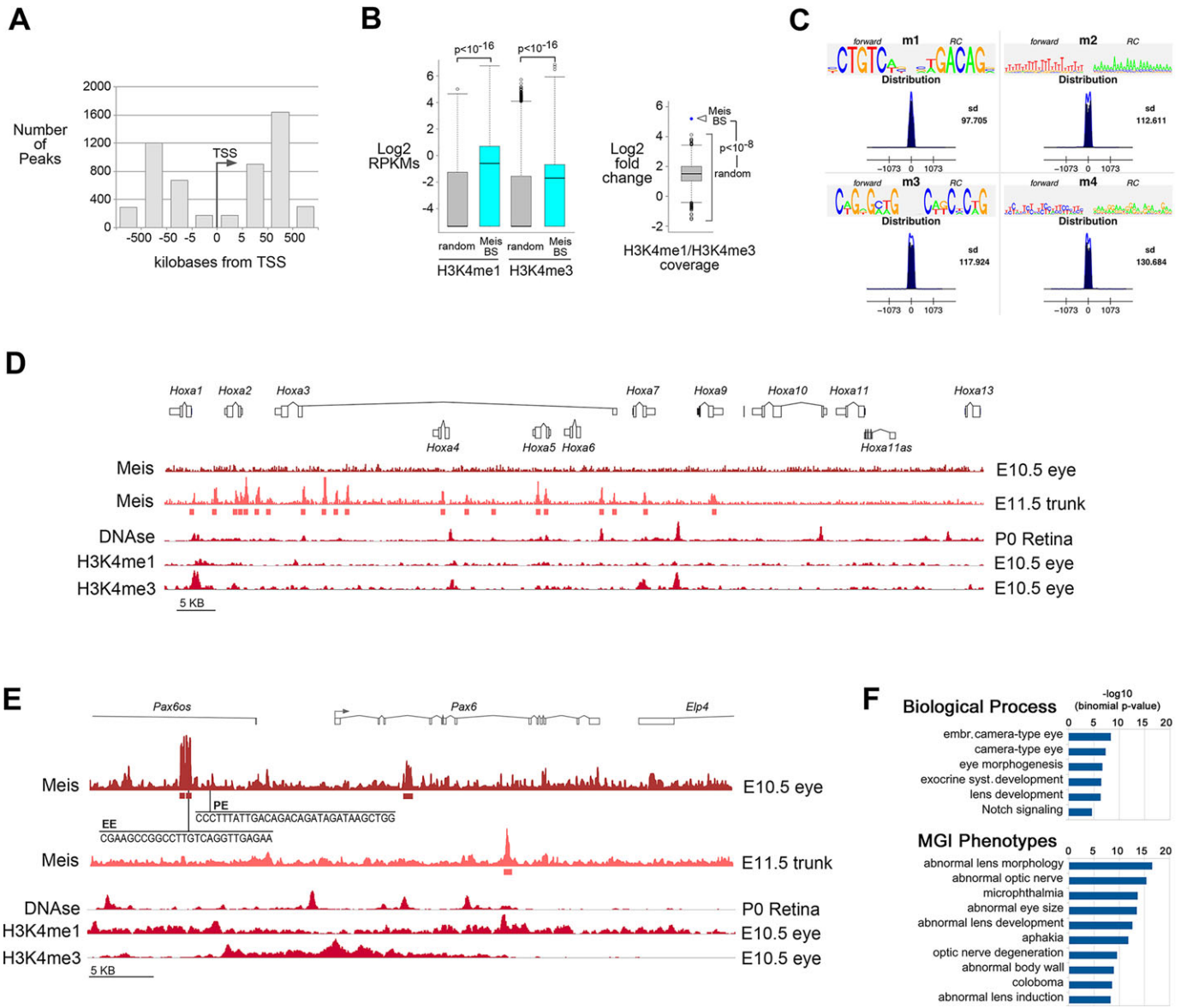

Fig. 5. ChIP-seq analysis of Meis1 function in the developing eye. (A) Distribution of Meis1 binding sites (BSs) by their position with respect to the nearest transcription start site (TSS). GREAT analysis (see Materials and Methods). (B) (Left) Distribution of H3K4me1 and H3K4me3 coverage in Meis BSs compared with that in a collection of randomly chosen equivalent genomic DNA segments. (Right) Comparison of the H3K4me1/H3K4me3 coverage ratio in Meis BSs (blue dot) versus that in a series of randomly chosen equivalent genomic DNA segments. (C) *De novo* identification of consensus sequences in the Meis BSs. Four motifs were identified (m1-m4). Forward and reverse complementary (RC) sequences and the distribution of the positions relative to the BS center are shown for each motif. (D,E) The *HoxA* complex and *Pax6* genomic regions showing the Meis1 ChIP-seq read profile from E10.5 eye (this study) and E11.5 trunk (Penkov et al., 2013), the P0 DNA-seq profile [from The ENCODE Project Consortium (2012), GEO:GSM1014188] and the H3K4me1 and H3K4me3 ChIP-seq profiles (this study, GEO GSE62786). Detected Meis1 BSs are shown by boxes below the read profiles. (E) The sequences bound by Meis in the ectoderm (EE) and pancreatic (PE) enhancers (Zhang et al., 2002, 2006) are indicated in the eye ChIP-seq profile of the *Pax6* genomic region. (F) The overrepresented 'biological process' and 'MGI phenotypes' GO classes are shown in order of significance by their binomial *P*-value.

association with enhancers involved in eye development, in contrast to what was observed in the embryonic trunk following a similar analysis (Penkov et al., 2013) as used here for comparison. Besides the 'eye development' categories, the 'Notch signaling' class appeared enriched in Meis1 BS-associated genes (Fig. 5F) in GO analysis.

Meis1 regulates the expression of Notch pathway genes and of selected genes involved in mammalian microphthalmia

To correlate the Meis1 BS pattern with actual gene expression regulation, we compared E10.5 wt and *Meis1*$^{-/-}$ eye cup transcriptomes by RNA-seq, identifying 406 downregulated and 242 upregulated transcripts (supplementary material Tables S1 and S2). The expression of transcripts encoding the core factors of the Notch pathway was extensively downregulated in *Meis1* mutants (Fig. 6A), indicating that this pathway is a major target of Meis1 regulation in the developing eye. To determine whether some of the genes encoding core components of the Notch pathway could be direct targets of Meis1, we examined the occurrence of Meis1 BSs in the enhancer-promoter units (EPUs) described in the ENCODE project (Shen et al., 2012). We found Meis BSs associated with the enhancer regions of *Notch2*, *Jag1*, *Hes2* and *Hes5*, coincident with enhancer histone marks in the E10.5 eye (supplementary material Fig. S3). A clear downregulation of *Hes5* mRNA, a major effector

Development (2015) 142, 3009-3020 doi:10.1242/dev.122176

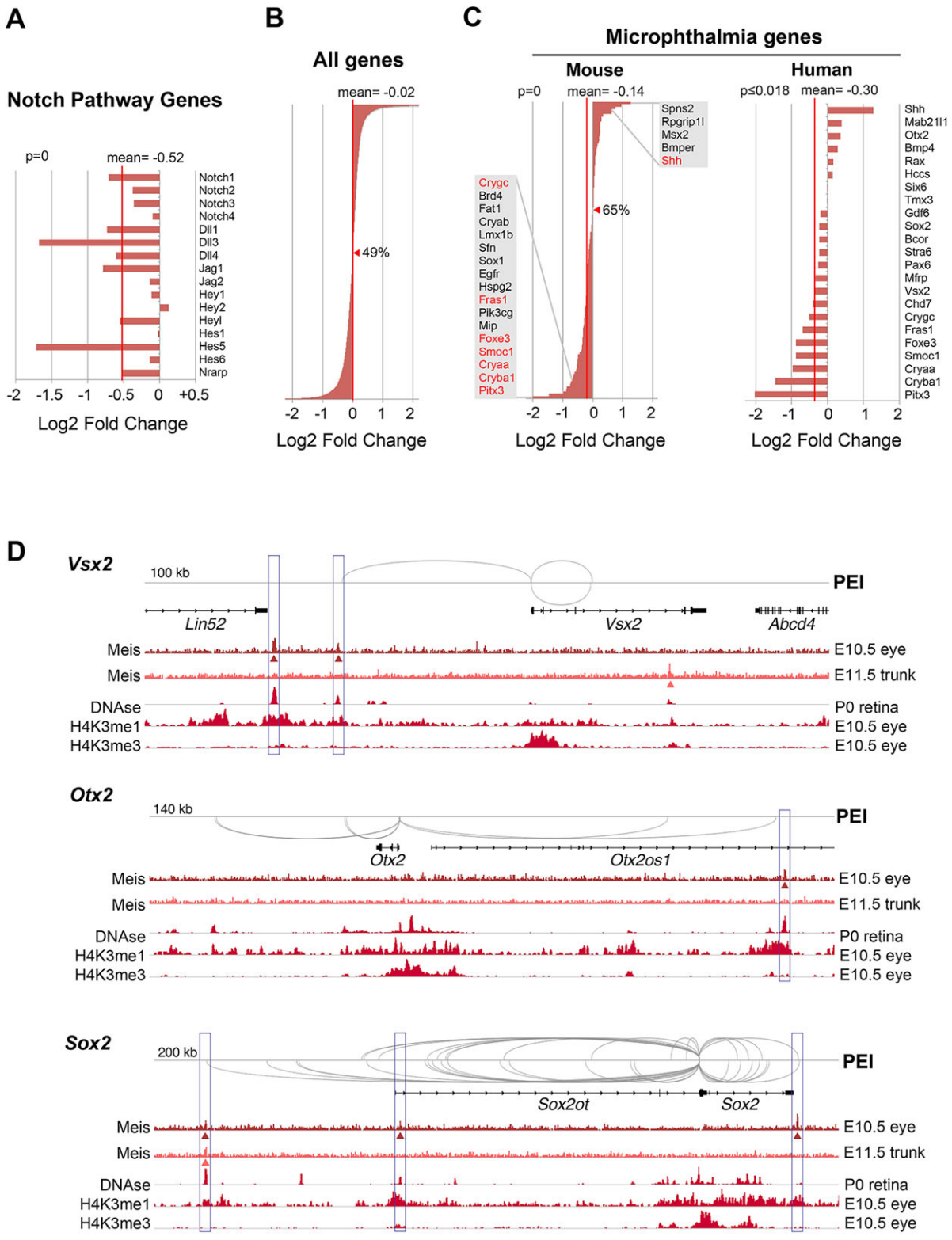

Fig. 6. Meis1 regulates components of the Notch signaling pathway and genes involved in microphthalmia. (A) RNA-seq expression level changes in genes encoding core components of the Notch signaling pathway detected in E10.5 *Meis1*$^{-/-}$ versus wt eyes. (B,C) Representations of changes in gene expression detected in *Meis1*$^{-/-}$ for all genes (B), mouse microphthalmia genes and mouse orthologs of human microphthalmia genes (C). Genes are ordered according to their expression change. A red line indicates the mean of expression variations. Gray boxes in C indicate genes with a $\log_2$ fold change >±0.5. Genes highlighted in red have a human ortholog associated with microphthalmia. The complete list of mouse orthologs of human genes analyzed in C is shown to the right. (A,C) p indicates the familywise error rate. (D) *Vsx2*, *Otx2* and *Sox2* genes showing their described promoter-enhancer interactions (PEI) according to Shen et al. (2012), the Meis1 ChIP-seq read profile from E10.5 eye (this study) and E11.5 trunk (Penkov et al., 2013), the P0 DNAse-seq profile [from The ENCODE Project Consortium (2012), GEO:GSM1014188] and the H3K4me1 and H3K4me3 ChIP-seq profiles (this study). Detected Meis1 BSs are shown by arrowheads below the read profiles. Boxes highlight the E10.5 eye Meis BS regions and their coincidence with histone modification marks and described enhancer-promoter interactions.

Development (2015) 142, 3009-3020 doi:10.1242/dev.122176

of Notch signaling, was further confirmed by comparative *in situ* hybridization (ISH) analysis in wt and *Meis1* mutants (Fig. 2D-F). These results suggest that Meis1 controls Notch pathway activity at various levels.

In addition, the association of Meis1 BSs with genes involved in eye size regulation, together with the reduced eye size of *Meis1* mutants, further suggested a relationship between Meis1 function and the direct or indirect regulation of microphthalmia genes. RNA-seq analysis that was focused on 121 mouse genes linked to microphthalmia confirmed this association (Fig. 6B,C). Interestingly, the human orthologs of the five most downregulated genes belonging to this class, *Pitx3*, *Smoc1*, *Cryba1*, *Cryaa* and *Foxe3*, have been associated with human microphthalmia (Fig. 6C) and a specific survey of all the mouse orthologs of human microphthalmia genes showed a very significant trend to downregulation in *Meis1* mutants (Fig. 6C). These results identify Meis1 as a major regulator of microphthalmia-associated genes.

To analyze possible direct targets within genes that change their expression levels, we determined the presence of Meis BSs in the EPUs of the 35 microphthalmia-associated genes that showed the strongest change in expression. We found that 11 out of these 35 genes contained one or more Meis BSs in their EPUs in coincidence with enhancer histone marks in E10.5 eyes (Fig. 6D; supplementary material Fig. S4; data not shown). Interestingly, 12 of the 35 genes showing altered expression and 8 of the 11 genes with Meis1 BSs in their EPUs encode TFs, including some of those more frequently associated with human microphthalmia (*Otx2*, *Vsx2*, *Sox2*; Fig. 6D). These results suggest that Meis1 controls eye size at various levels but predominantly by orchestrating the regulation of microphthalmia-associated TFs.

Meis1 is required to sharpen the boundaries between the different eye territories

Because eye development gene classes were overrepresented in Meis1 ChIP-seq analysis (Fig. 5F), developmental processes other than neurogenesis were likely to be affected in *Meis1* mutant eyes. To test this possibility we analyzed the distribution of well-established markers of eye patterning. Although most of these markers were detected, their distribution was generally shifted and with blurred boundaries: for example, the border between Pax2, a marker of the proximal eye (optic stalk), and Pax6, a marker of the distal eye, was distally shifted, with a clear increase in Pax2 expression in *Meis1* mutants versus wt embryos (Fig. 7A-F); this is also in agreement with the enhanced expression of Shh in mutants (Fig. 6C), which is known to expand the optic stalk. Similarly, Otx2, an RPE marker (Martinez-Morales et al., 2004), was abnormally extended in the ventrodistal retina (Fig. 7G-I), in accordance with RNA-seq analysis and the presence of Meis BSs in its locus (Fig. 6C,D). The $Otx1^{+}$ peripheral retina invaded the $Vsx2^{+}$ central retina (Fig. 7J-O), again in agreement with our RNA-seq and ChIP-seq analysis indicating that Meis1 might activate *Vsx2* (Fig. 6C,D). Patterning along the dorsoventral axis was also abnormal, with an expansion of the $Tbx5^{+}$ dorsal region and a reduction of the $Vax2^{+}$ ventral retina, whereas the expression of *Foxd1*, a temporal retinal marker, was considerably reduced (Fig. 7P-X). Notably, blurring of all boundaries was dose-dependent, as these defects were milder in $Meis1^{+/-}$ eyes (Fig. 7).

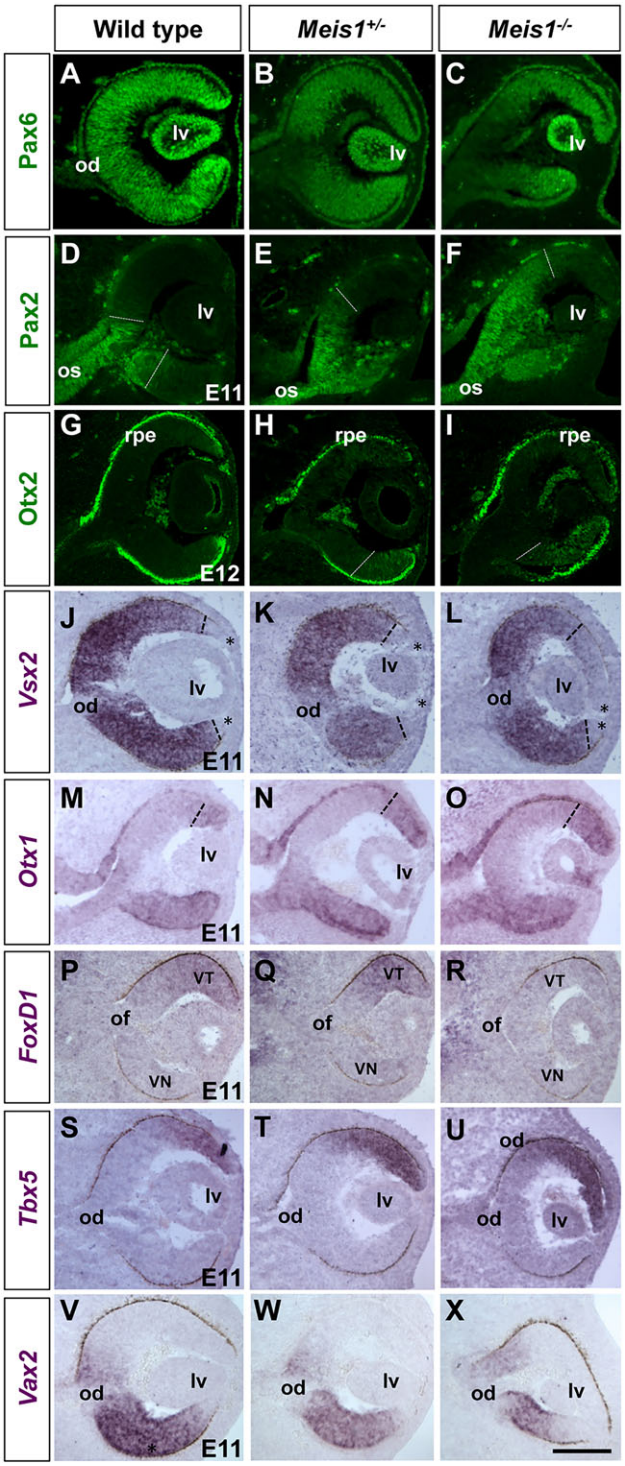

Fig. 7. *Meis1* is required to define proper patterning of the optic cup along its principal axes. Frontal (A-O,S-X) and horizontal (P-R) cryostat sections of E11 wt, $Meis1^{+/-}$ and $Meis1^{-/-}$ optic cups processed for the indicated markers. Note the allele-dependent expression shift of the various markers in *Meis1* mutant optic cups. Asterisks (J-L) indicate the tip of the ciliary margins. Dashed lines delineate the extent of marker staining. lv, lens vesicle; od, optic disc; of, optic fissure; os, optic stalk; rpe, retinal pigmented epithelium; VN, ventronasal; VT, ventrotemporal. Scale bar: 25 µm.

DISCUSSION

In mammals, *Meis1* is crucial for the formation of the heart, vasculature and hematopoietic system (Azcoitia et al., 2005; Hisa et al., 2004). During the development of these structures, as well as that of the limbs, Meis1 acts as a co-factor for Hox proteins, often in cooperation with the related Pbx TFs (Penkov et al., 2013). Our study demonstrates that Meis1 is also crucial for the progressive

Development (2015) 142, 3009-3020 doi:10.1242/dev.122176

formation of the eye, but, in this case, its function is mediated by Hox/Pbx-independent BSs on the DNA. In the absence of *Meis1*, the expression of the main patterning determinants of the optic cup is altered and the boundaries between the proximodistal, dorsoventral and nasotemporal domains of the cup are shifted or blurred. Retinal neurogenesis is also affected because Meis1, directly or indirectly, controls the expression of components of the neurogenic cascade mediated by the Notch receptor. Furthermore, Meis1 is required for the expression of a set of genes involved in mammalian microphthalmia. Accordingly, *Meis1* haploinsufficient adult mice present morphological and functional defects characteristic of this congenital defect. Therefore, our data, together with previous studies showing that *Meis1* controls lens development and Ccnd1-mediated retinal proliferation (Bessa et al., 2008; Heine et al., 2008; Zhang et al., 2002), indicate that *Meis1* is a global regulator of eye development.

At least in mammals, this key function does not seem to be shared by the related *Meis2* or *Meis3*. *Meis3* is expressed in the eye only when the first retinal ganglion cells begin to differentiate (Gray et al., 2004). Both *Meis2* and *Meis1* contribute to lens specification by binding to the same BS present in a lens-specific enhancer of the *Pax6* locus (Zhang et al., 2002), but only *Meis1* is strongly and continuously expressed in the retinal neuroepithelium, according to our data and the distribution previously reported (Zhang et al., 2002). *Meis2*$^{-/-}$ mice have no evident early eye alterations (M.T., unpublished observations), suggesting that the reported *Meis2* expression in the optic vesicle (Heine et al., 2008) is either too transient to be consistently detected and/or dispensable in the gene regulatory network that controls early eye formation. This predominant role of *Meis1* in the mammalian eye primordium differs from that reported in chick and fish, in which alteration of *Meis2* levels also perturbs eye development (Conte et al., 2010; Heine et al., 2008). Furthermore, in contrast to its role in zebrafish where it is limited to neurogenesis (Bessa et al., 2008), *Meis1* is also crucial for patterning and neuronal differentiation in the mouse retina. This latter function is supported by the maintenance of Meis1 expression in differentiated neurons, which are very much reduced in number in *Meis1*$^{-/-}$ mouse embryos. A similar role has been observed in chick, in which interference with Meis function compromises the appearance of retinal differentiation markers (Heine et al., 2008), including *Foxn4*, a TF directly regulated by Meis1 and important for the generation of horizontal and amacrine neurons (Islam et al., 2013). As shown here, Meis2 rescues Meis1 deficiency in the vascular system, indicating that the two proteins are functionally similar and can show redundancy during eye development. Differential evolution of the regulatory elements controlling *Meis1* and *Meis2* expression, rather than Meis1/2 protein functional specialization, might thus underlie their different requirement in fish, avian and mammalian eye development.

Our expression and genomic analyses indicate that Meis1 must act upstream in the gene regulatory network controlling eye formation, as several of its targets are themselves TFs at the core of the network, such as Sox2, Otx2 and Pax6 (Beccari et al., 2013). Genetic inactivation of *Meis1* does not prevent the formation of the eye primordium, although it has, however, a fuzzy pattern. This 'fuzziness' affects its main tissues – optic stalk, neural retina and RPE – as well as its entire axes, indicating that *Meis1* is crucial to consolidate boundaries between the different eye domains. Meis1 could, for example, render the activity of each of the tissue determinant genes [e.g. Otx2 for the RPE (Martinez-Morales et al., 2001)] more efficient. There are various and not mutually exclusive mechanisms by which this could occur. In a view based around its cooperation with Hox/Pbx in the trunk (Duboule, 2007; Penkov et al., 2013), Meis1 could act as a co-factor with an as yet undefined predominant partner, perhaps binding to the m2-m3 core sequence that we have identified. This interaction would make the putative factor more efficient, allowing the correct expression of target genes. Alternatively, Meis1 could interact with a wide variety of TFs in the eye, including its own putative targets such as Sox2, Pax6 and Otx2, reinforcing their activity. The latter possibility is supported by the observation that the related Meis2 has been shown to interact at least with Otx2, Pax3, Pax6 and Pax7 (Agoston et al., 2014, 2012; Agoston and Schulte, 2009). Alternatively, and based on the predominant presence of a 'Meis1-only' targeted sequence (m1, Fig. 5) in the eye chromatin, we favor the hypothesis that Meis1 directly binds on enhancers of many determinant genes. Its binding would be necessary to achieve sufficient levels of target expression, and indispensable for regulating the extent of each domain. This mechanism could be illustrated by possible direct regulation by Meis1 of Pax6 in the retina and the establishment of proximodistal patterning of the optic vesicle. Indeed, the boundary between the proximal and distal optic vesicle is known to depend on a cross-regulatory loop between Pax6 expressed distally and Pax2 expressed proximally (Schwarz et al., 2000). We have identified a Meis1 BS on a *Pax6* enhancer that is different to that known to mediate lens development (Zhang et al., 2002). In the absence of *Meis1*, retinal Pax6 expression is strongly reduced, probably allowing *Pax2* upregulation. This should result in a weak cross-repressive loop between the two TFs and thus in a shifted proximodistal boundary, which is indeed observed in *Meis1* mutant embryos. This mechanism could be reinforced by a possible direct repression of Meis1, as we identified by ChIP-seq Meis BSs in the *Pax2* locus. Similar considerations could apply for other TFs known to act in a cross-regulatory loop during boundary establishment, as with FoxG1 and FoxD1 in the specification of the nasotemporal domains of the retina (Hatini et al., 1994; Huh et al., 1999). Notably, we identified by ChIP-seq Meis BSs also in the *Foxd1* locus.

A similar potential direct regulation could also be relevant in the control of components of the Notch signaling pathway, including the Notch2 receptor and the Notch signaling effectors Hes2 and Hes5. For other members of the pathway, the decreased expression identified in our RNA-seq comparison might instead be indirect. Nevertheless, whether direct or not, the poor Notch pathway activation, in conjunction with decreased expression of *Ccnd1* and other microphthalmia-associated genes, could explain the *Meis1*$^{-/-}$ microphthalmic phenotype. Indeed, Notch signaling controls the number of progenitors entering retinal differentiation: loss of Notch function forestalls retinal neurogenesis (Jadhav et al., 2006), whereas abnormal Notch receptor activation transiently increases retinal proliferation and differentiation (Esteve et al., 2011). Notably, Meis1 action on the Notch pathway and on microphthalmia-related genes could be linked since *Sox1*, *Sox2* and Notch signaling have been shown to regulate each other's activity in various contexts (Genethliou et al., 2009; Kan et al., 2004; Neves et al., 2011). Most notably, Sox2 regulates the Notch signaling pathway in retinal progenitor cells in a concentration-dependent manner, so that the levels of Sox2 directly correlate with the levels of Notch1 (Taranova et al., 2006), a correlation that we have also observed between *Meis1* levels and *Hes5* expression.

Our RNA-seq analysis reveals a strong association between Meis1 function and genes linked to microphthalmia. As expected from the use of complete E10.5 eye cups, we identified genes expressed only in the lens, such as the TF *Foxe3* and the crystallins (Graw, 2009), or in the neural retina, including the TF *Vsx2* and

Development (2015) 142, 3009-3020 doi:10.1242/dev.122176

Smoc1 (Liu et al., 1994; Okada et al., 2011), or in both, such as *Sox1/2* and *Otx2* (Fuhrmann, 2010; Lang, 2004). This finding not only supports a pleiotropic function of Meis1 in eye formation but also indicates a direct role of Meis1 in the development of the retinal neuroepithelium. Our analysis of mutants with a conditional rescue of *Meis1* expression in the vasculature indicates that the microphthalmia observed is unlikely to derive from abnormal vasculature formation. The relative impact of *Meis1* loss-of-function on the lens or retina in the microphthalmic phenotype cannot be precisely dissected in our analysis. However, *Meis1* haploinsufficiency in the adult mouse eye has no consequence for blood vessel or lens development but it affects the expression of patterning and neurogenic genes, indicating that the retinal neuroepithelium is more sensitive to the levels of *Meis1* expression, directly implicating *Meis1* in retina development.

In conclusion, our data support that *Meis1* has a crucial and previously unreported role in integrating patterning and neurogenesis of the developing eye through the regulation of signaling pathways and patterning genes. *Meis1* seems to be at the core of a genetic network implicated in human microphthalmia, itself representing an additional candidate for syndromic cases associated with this ocular malformation. In this respect, eye developmental defects, including bilateral microphthalmia, have been linked to alterations in chromosome 2 (Waters et al., 1993; Weaver et al., 1991), at a location that may include the extensive *MEIS1* regulatory region (Royo et al., 2012), raising the possibility that reduced MEIS1 levels could contribute to the phenotypic traits.

MATERIALS AND METHODS

Animals

Meis1a heterozygous mice were generated as described (Azcoitia et al., 2005). Embryos were obtained from timed (vaginal plug as E0.5) mating of *Meis1a*$^{+/-}$ mice or outbred CD1 mice. Animals were treated according to institutional or national guidelines for the use of animals in scientific research.

BrdU incorporation

BrdU (10 mg/ml; Roche) was injected (50 µg/g body weight) into pregnant mice intraperitoneally. Embryos were sacrificed and collected 1 h later.

TUNEL

Staining was performed using the In Situ Cell Death Detection Kit (Roche) on cryosections following the manufacturer's instructions.

In situ hybridization

E10.5-13.5 embryos were immersion fixed in 4% paraformaldehyde in PBS for 3 h. Tissue was processed for cryosectioning in the frontal or horizontal plane and ISH was performed as previously described (Causeret et al., 2004) using the following digoxigenin-labeled mouse-specific antisense riboprobes were used: *Fgf15*, *Ccnd1*, *Hes5*, *Tbx5*, *Vax2*, *Foxd1*, *Otx1*, *Vsx2*.

Immunohistochemistry

Cryosections were incubated with 0.1% Triton X-100 in PBS (PBT) and immunofluorescence was performed in PBT with 1% normal goat serum. For Otx2, Pax6 and Pax2 staining, sections were heated at 110°C for 2 min in 10 mM citrate buffer (pH 6) using a decloaking chamber (Biocare Medical). The following primary antibodies were used (at 1:1000 unless stated otherwise): rabbit anti-Meis1a/2a (Mercader et al., 2005), anti-Otx2 (Abcam, ab21990), anti-cleaved caspase 3 (Cell Signaling, 9661), anti-Pax2 (Invitrogen, 71-6000), anti-Pax6 (Covance, PRB278P); mouse anti-phospho-histone H3 (Millipore, 06-570), anti-BrdU [1:4000; DSHB, G3G4(AntiBrdUrd)], anti-Isl1/2 (1:500; DSHB, 39.4D5) and anti-Tuj1 (βIII tubulin, Babco, MMS-435P). Secondary antibodies were conjugated to Alexa 488 or Alexa 594 (1:1000; Molecular Probes). Counterstaining was with DAPI (1 µg/ml; Vector Labs).

RNA-seq

For RNA-seq library production, RNA of intact E10.5 optic cups (thus including the lens) from eight homozygous and wt embryos (out of 41 embryos from seven litters) was isolated using standard procedures, quantified (260 nm in a NanoDrop) and checked for integrity (Agilent Bioanalyzer). Total RNA was processed with the TruSeq RNA Sample Preparation v2 Kit (Illumina) to construct index-tagged cDNA libraries. The quality, quantity and the size distribution of the Illumina libraries were determined using the DNA-1000 Kit (Agilent Bioanalyzer). Prepared cDNA libraries were applied to an Illumina flow cell for cluster generation (TruSeq SR Cluster Kit V2 cBot, Illumina) and sequence-by-synthesis single reads of 75 bp using the TruSeq SBS Kit v5 (Illumina) were generated on the Genome Analyzer IIx (Illumina) following the standard RNA sequencing protocol. Sequencing adaptor contaminations were removed from reads using cutadapt software (http://code.google.com/p/cutadapt/) and the resulting reads were mapped and quantified on the transcriptome (Ensembl gene build 70) using RSEM v1.2.3 (Li and Dewey, 2011). Only genes with at least five counts per million in at least one sample were considered for statistical analysis. Data were then normalized and differential expression tested using the Bioconductor package edgeR (Robinson et al., 2010). Genes were considered differentially expressed when they presented a fold change ≥40%. Data were analyzed using Gene set enrichment and Ingenuity pathway software (Biobase International). Mouse microphthalmia genes were obtained by searching the Jackson Laboratory Mouse Genome Informatics database for the term 'microphthalmia' in the field 'mouse phenotypes and mouse models of human disease' of the 'genes and markers' query. Data are deposited in the NCBI GEO database under accession number GSE62786.

ChIP-seq

ChIP assays to determine the histone methylation marks were performed using ∼100 eyes from E10.5 mouse embryos. Chromatin was cross-linked with 1% formaldehyde for 15 min and fragmented to obtain DNA in the range 200-500 bp. DNA was divided in three pools (of 10 µg) and precipitated with 2 µg anti-H3K4me1 (CS-037-100, Diagenode) or anti-H3K4me3 (pAB-033-050, Diagenode). Immunoprecipitated DNA was purified with QIAquick columns (Qiagen). Data are deposited in the NCBI GEO database under accession number GSE62786. ChIP data for Meis1 were obtained from ∼200 eyes of E10.5 CD1 embryos. Two pools of ∼20 µg total chromatin were immunoprecipitated with 4 µg anti-Meis1 antibody (Mercader et al., 2005) and the immunoprecipitated DNA was purified and pooled together. ChIP-seq and bioinformatic processing were performed as described (Penkov et al., 2013). Chromatin was cross-linked with 1% formaldehyde for 15 min and fragmented to 300-500 bp. Data have been deposited in the NCBI GEO database under accession number GSE62786. Annotation of Meis1 BSs and identification of Meis1 BS-associated genes or overrepresentation in GO and phenotype-association databases was performed with the 'genomic regions enrichment of annotations tool' (GREAT) (McLean et al., 2010). For the identified peaks, '*de novo* motif discovery' was run to identify consensus sequences enriched in the selected regions versus the whole genome using rGADEM (Li, 2009).

Morphometric and functional analysis of the eye

The visual acuity and eye morphology of *Meis1a* mutant mice were evaluated at 15 weeks of age by virtual optokinetic drum, Scheimpflug imaging, OCT and laser interference biometry (LIB). For LIB and OCT, the eyes were treated with 1% atropine to ensure pupil dilation and mice were further anesthetized with 137 mg ketamine and 6.6 mg xylazine per kg body weight. For all tests, previously published protocols were followed: virtual drum vision test (Prusky et al., 2004), Scheimpflug imaging (Puk et al., 2013a), OCT (Puk et al., 2013b) and LIB (Puk et al., 2006).

Quantification and statistical analysis

Area measurements and cell counting were performed with a Leica DM 5000M fluorescence microscope and a Leica DFC 500 camera. All

Development (2015) 142, 3009-3020 doi:10.1242/dev.122176

statistical analysis was performed using a minimum of 3 or 6 embryos or eyes per genotype, using ImageJ software (NIH). Differences between calculated averages were considered significant when $P<0.05$ by Student's *t*-test. For each of the ISH probes or immunohistochemical markers used in this study, analysis was performed on a minimum of three embryos for each genotype. For each embryo, all sections from both eyes were photographed and compared using sections at the same axial level.

Acknowledgements

We thank J. R. Martinez-Morales (CBD) for critically reading the manuscript; V. García for mouse care; the CMBSO Genomics Facility for help with ChIP-seq; and M. J. Gómez-Rodriguez, Manuel Gómez and F. Sánchez-Cabo (CNIC) for bioinformatics analyses. The CNIC Genomics Unit performed the RNA-seq procedures.

Competing interests

The authors declare no competing or financial interests.

Author contributions

P.B., M.T. and S.M. conceived the study; J.G. and M.H.d.A. conceived the phenotypic tests; S.M., M.G.-L., L.B., L.C., R.D., O.P., O.A. and M.J.M.-B. performed experiments; S.M., L.B., O.B., J.G., D.M.-S.M., C.T., J.L.G.-S., F.C., M.T. and P.B. analyzed the data; M.T. and P.B. wrote the paper. All authors approved the manuscript.

Funding

This work was supported by grants from the Spanish Ministry of Economy and Competitiveness (MINECO) [BFU2010-16031; BFU2013-43213-P, supported by FEDER Funds], the CIBERER, Instituto de Salud Carlos III (ISCIII) to P.B. and an Institutional Grant from the Fundación Ramon Areces; by MINECO [BFU2012-31086] and ISCIII [RD12/0019/0005] to M.T.; by Comunidad Autonoma de Madrid (CAM) [S2010/BMD-2315] to P.B. and M.T.; by MINECO [BFU2013-41322-P] and Andalusian Government [BIO-396] to J.L.G.-S.; and by MINECO [BFU2014-55738-REDT] to P.B., J.L.G.-S. and F.C. M.G.-L. was supported by a grant from the CONACyT. O.B. is supported by an Australian Research Council Discovery Early Career Researcher Award-DECRA [DE140101962]. The CNIC is supported by MINECO and the Pro-CNIC Foundation.

Supplementary material

Supplementary material available online at
http://dev.biologists.org/lookup/suppl/doi:10.1242/dev.122176/-/DC1

References

Abouzeid, H., Boisset, G., Favez, T., Youssef, M., Marzouk, I., Shakankiry, N., Bayoumi, N., Descombes, P., Agosti, C., Munier, F. L. et al. (2011). Mutations in the SPARC-related modular calcium-binding protein 1 gene, SMOC1, cause waardenburg anophthalmia syndrome. *Am. J. Hum. Genet.* **88**, 92-98.

Agoston, Z. and Schulte, D. (2009). Meis2 competes with the Groucho co-repressor Tle4 for binding to Otx2 and specifies tectal fate without induction of a secondary midbrain-hindbrain boundary organizer. *Development* **136**, 3311-3322.

Agoston, Z., Li, N., Haslinger, A., Wizenmann, A. and Schulte, D. (2012). Genetic and physical interaction of Meis2, Pax3 and Pax7 during dorsal midbrain development. *BMC Dev. Biol.* **12**, 10.

Agoston, Z., Heine, P., Brill, M. S., Grebbin, B. M., Hau, A. C., Kallenborn-Gerhardt, W., Schramm, J., Gotz, M. and Schulte, D. (2014). Meis2 is a Pax6 co-factor in neurogenesis and dopaminergic periglomerular fate specification in the adult olfactory bulb. *Development* **141**, 28-38.

Azcoitia, V., Aracil, M., Martínez-A, C. and Torres, M. (2005). The homeodomain protein Meis1 is essential for definitive hematopoiesis and vascular patterning in the mouse embryo. *Dev. Biol.* **280**, 307-320.

Bardakjian, T. M. and Schneider, A. (2011). The genetics of anophthalmia and microphthalmia. *Curr. Opin. Ophthalmol.* **22**, 309-313.

Beccari, L., Marco-Ferreres, R. and Bovolenta, P. (2013). The logic of gene regulatory networks in early vertebrate forebrain patterning. *Mech. Dev.* **130**, 95-111.

Bessa, J., Gebelein, B., Pichaud, F., Casares, F. and Mann, R. S. (2002). Combinatorial control of Drosophila eye development by eyeless, homothorax, and teashirt. *Genes Dev.* **16**, 2415-2427.

Bessa, J., Tavares, M. J., Santos, J., Kikuta, H., Laplante, M., Becker, T. S., Gomez-Skarmeta, J. L. and Casares, F. (2008). meis1 regulates cyclin D1 and c-myc expression, and controls the proliferation of the multipotent cells in the early developing zebrafish eye. *Development* **135**, 799-803.

Bovolenta, P., Mallamaci, A., Briata, P., Corte, G. and Boncinelli, E. (1997). Implication of OTX2 in pigment epithelium determination and neural retina differentiation. *J. Neurosci.* **17**, 4243-4252.

Capellini, T. D., Zappavigna, V. and Selleri, L. (2011). Pbx homeodomain proteins: TALEnted regulators of limb patterning and outgrowth. *Dev. Dyn.* **240**, 1063-1086.

Causeret, F., Hidalgo-Sanchez, M., Fort, P., Backer, S., Popoff, M. R., Gauthier-Rouviere, C. and Bloch-Gallego, E. (2004). Distinct roles of Rac1/Cdc42 and Rho/Rock for axon outgrowth and nucleokinesis of precerebellar neurons toward netrin 1. *Development* **131**, 2841-2852.

Conte, I., Carrella, S., Avellino, R., Karali, M., Marco-Ferreres, R., Bovolenta, P. and Banfi, S. (2010). miR-204 is required for lens and retinal development via Meis2 targeting. *Proc. Natl. Acad. Sci. USA* **107**, 15491-15496.

Duboule, D. (2007). The rise and fall of Hox gene clusters. *Development* **134**, 2549-2560.

Erickson, T., French, C. R. and Waskiewicz, A. J. (2010). Meis1 specifies positional information in the retina and tectum to organize the zebrafish visual system. *Neural Dev.* **5**, 22.

Esteve, P. and Bovolenta, P. (2006). Secreted inducers in vertebrate eye development: more functions for old morphogens. *Curr. Opin. Neurobiol.* **16**, 13-19.

Esteve, P., Sandonìs, A., Cardozo, M., Malapeira, J., Ibañez, C., Crespo, I., Marcos, S., Gonzalez-Garcia, S., Toribio, M. L., Arribas, J. et al. (2011). SFRPs act as negative modulators of ADAM10 to regulate retinal neurogenesis. *Nat. Neurosci.* **14**, 562-569.

Fantes, J., Ragge, N. K., Lynch, S.-A., McGill, N. I., Collin, J. R., Howard-Peebles, P. N., Hayward, C., Vivian, A. J., Williamson, K., van Heyningen, V. et al. (2003). Mutations in SOX2 cause anophthalmia. *Nat. Genet.* **33**, 461-463.

Ferda Percin, E., Ploder, L. A., Yu, J. J., Arici, K., Horsford, D. J., Rutherford, A., Bapat, B., Cox, D. W., Duncan, A. M. V., Kalnins, V. I. et al. (2000). Human microphthalmia associated with mutations in the retinal homeobox gene CHX10. *Nat. Genet.* **25**, 397-401.

Fuhrmann, S. (2010). Eye morphogenesis and patterning of the optic vesicle. *Curr. Top. Dev. Biol.* **93**, 61-84.

Gallardo, M. E., Rodriguez De Cordoba, S., Schneider, A. S., Dwyer, M. A., Ayuso, C. and Bovolenta, P. (2004). Analysis of the developmental SIX6 homeobox gene in patients with anophthalmia/microphthalmia. *Am. J. Med. Genet. A* **129A**, 92-94.

Genethliou, N., Panayiotou, E., Panayi, H., Orford, M., Mean, R., Lapathitis, G., Gill, H., Raoof, S., De Gasperi, R., Elder, G. et al. (2009). SOX1 links the function of neural patterning and Notch signalling in the ventral spinal cord during the neuron-glial fate switch. *Biochem. Biophys. Res. Commun.* **390**, 1114-1120.

Glaser, T., Jepeal, L., Edwards, J. G., Young, S. R., Favor, J. and Maas, R. L. (1994). PAX6 gene dosage effect in a family with congenital cataracts, aniridia, anophthalmia and central nervous system defects. *Nat. Genet.* **7**, 463-471.

Graw, J. (2009). Mouse models of cataract. *J. Genet.* **88**, 469-486.

Gray, P. A., Fu, H., Luo, P., Zhao, Q., Yu, J., Ferrari, A., Tenzen, T., Yuk, D.-I., Tsung, E. F., Cai, Z. et al. (2004). Mouse brain organization revealed through direct genome-scale TF expression analysis. *Science* **306**, 2255-2257.

Hatini, V., Tao, W. and Lai, E. (1994). Expression of winged helix genes, BF-1 and BF-2, define adjacent domains within the developing forebrain and retina. *J. Neurobiol.* **25**, 1293-1309.

Heine, P., Dohle, E., Bumsted-O'Brien, K., Engelkamp, D. and Schulte, D. (2008). Evidence for an evolutionary conserved role of homothorax/Meis1/2 during vertebrate retina development. *Development* **135**, 805-811.

Hisa, T., Spence, S. E., Rachel, R. A., Fujita, M., Nakamura, T., Ward, J. M., Devor-Henneman, D. E., Saiki, Y., Kutsuna, H., Tessarollo, L. et al. (2004). Hematopoietic, angiogenic and eye defects in Meis1 mutant animals. *EMBO J.* **23**, 450-459.

Huh, S., Hatini, V., Marcus, R. C., Li, S. C. and Lai, E. (1999). Dorsal-ventral patterning defects in the eye of BF-1-deficient mice associated with a restricted loss of shh expression. *Dev. Biol.* **211**, 53-63.

Indrieri, A., Conte, I., Chesi, G., Romano, A., Quartararo, J., Tatè, R., Ghezzi, D., Zeviani, M., Goffrini, P., Ferrero, I. et al. (2013). The impairment of HCCS leads to MLS syndrome by activating a non-canonical cell death pathway in the brain and eyes. *EMBO Mol. Med.* **5**, 280-293.

Islam, M. M., Li, Y., Luo, H., Xiang, M. and Cai, L. (2013). Meis1 regulates Foxn4 expression during retinal progenitor cell differentiation. *Biol. Open* **2**, 1125-1136.

Jadhav, A. P., Cho, S.-H. and Cepko, C. L. (2006). Notch activity permits retinal cells to progress through multiple progenitor states and acquire a stem cell property. *Proc. Natl. Acad. Sci. USA* **103**, 18998-19003.

Kan, L., Israsena, N., Zhang, Z., Hu, M., Zhao, L.-R., Jalali, A., Sahni, V. and Kessler, J. A. (2004). Sox1 acts through multiple independent pathways to promote neurogenesis. *Dev. Biol.* **269**, 580-594.

Lang, R. A. (2004). Pathways regulating lens induction in the mouse. *Int. J. Dev. Biol.* **48**, 783-791.

Li, L. (2009). GADEM: a genetic algorithm guided formation of spaced dyads coupled with an EM algorithm for motif discovery. *J. Comput. Biol.* **16**, 317-329.

Li, B. and Dewey, C. N. (2011). RSEM: accurate transcript quantification from RNA-Seq data with or without a reference genome. *BMC Bioinformatics* **12**, 323.

Liu, I. S. C., Chen, J.-D., Ploder, L., Vidgen, D., van der Kooy, D., Kalnins, V. I. and McInnes, R. R. (1994). Developmental expression of a novel murine homeobox gene (Chx10): evidence for roles in determination of the neuroretina and inner nuclear layer. *Neuron* **13**, 377-393.

Longobardi, E., Penkov, D., Mateos, D., De Florian, G., Torres, M. and Blasi, F. (2014). Biochemistry of the tale transcription factors PREP, MEIS, and PBX in vertebrates. *Dev. Dyn.* **243**, 59-75.
Mallo, M. and Alonso, C. R. (2013). The regulation of Hox gene expression during animal development. *Development* **140**, 3951-3963.
Martinez-Morales, J. R., Signore, M., Acampora, D., Simeone, A. and Bovolenta, P. (2001). Otx genes are required for tissue specification in the developing eye. *Development* **128**, 2019-2030.
Martinez-Morales, J. R., Rodrigo, I. and Bovolenta, P. (2004). Eye development: a view from the retina pigmented epithelium. *Bioessays* **26**, 766-777.
Martinez-Morales, J.-R., Del Bene, F., Nica, G., Hammerschmidt, M., Bovolenta, P. and Wittbrodt, J. (2005). Differentiation of the vertebrate retina is coordinated by an FGF signaling center. *Dev. Cell* **8**, 565-574.
McLean, C. Y., Bristor, D., Hiller, M., Clarke, S. L., Schaar, B. T., Lowe, C. B., Wenger, A. M. and Bejerano, G. (2010). GREAT improves functional interpretation of cis-regulatory regions. *Nat. Biotechnol.* **28**, 495-501.
Mercader, N., Leonardo, E., Azpiazu, N., Serrano, A., Morata, G., Martinez, C. and Torres, M. (1999). Conserved regulation of proximodistal limb axis development by Meis1/Hth. *Nature* **402**, 425-429.
Mercader, N., Tanaka, E. M. and Torres, M. (2005). Proximodistal identity during vertebrate limb regeneration is regulated by Meis homeodomain proteins. *Development* **132**, 4131-4142.
Mercader, N., Selleri, L., Criado, L. M., Pallares, P., Parras, C., Cleary, M. L. and Torres, M. (2009). Ectopic Meis1 expression in the mouse limb bud alters P-D patterning in a Pbx1-independent manner. *Int. J. Dev. Biol.* **53**, 1483-1494.
Morcillo, J., Martinez-Morales, J. R., Trousse, F., Fermin, Y., Sowden, J. C. and Bovolenta, P. (2006). Proper patterning of the optic fissure requires the sequential activity of BMP7 and SHH. *Development* **133**, 3179-3190.
Morleo, M., Pramparo, T., Perone, L., Gregato, G., Le Caignec, C., Mueller, R. F., Ogata, T., Raas-Rothschild, A., de Blois, M. C., Wilson, L. C. et al. (2005). Microphthalmia with linear skin defects (MLS) syndrome: clinical, cytogenetic, and molecular characterization of 11 cases. *Am. J. Med. Genet. A* **137A**, 190-198.
Neves, J., Parada, C., Chamizo, M. and Giraldez, F. (2011). Jagged 1 regulates the restriction of Sox2 expression in the developing chicken inner ear: a mechanism for sensory organ specification. *Development* **138**, 735-744.
Ng, D., Thakker, N., Corcoran, C. M., Donnai, D., Perveen, R., Schneider, A., Hadley, D. W., Tifft, C., Zhang, L., Wilkie, A. O. M. et al. (2004). Oculofaciocardiodental and Lenz microphthalmia syndromes result from distinct classes of mutations in BCOR. *Nat. Genet.* **36**, 411-416.
Okada, I., Hamanoue, H., Terada, K., Tohma, T., Megarbane, A., Chouery, E., Abou-Ghoch, J., Jalkh, N., Cogulu, O., Ozkinay, F. et al. (2011). SMOC1 is essential for ocular and limb development in humans and mice. *Am. J. Hum. Genet.* **88**, 30-41.
Pasutto, F., Sticht, H., Hammersen, G., Gillessen-Kaesbach, G., Fitzpatrick, D. R., Nürnberg, G., Brasch, F., Schirmer-Zimmermann, H., Tolmie, J. L., Chitayat, D. et al. (2007). Mutations in STRA6 cause a broad spectrum of malformations including anophthalmia, congenital heart defects, diaphragmatic hernia, alveolar capillary dysplasia, lung hypoplasia, and mental retardation. *Am. J. Hum. Genet.* **80**, 550-560.
Penkov, D., Mateos San Martín, D., Fernandez-Díaz, L. C., Rosselló, C. A., Torroja, C., Sánchez-Cabo, F., Warnatz, H. J., Sultan, M., Yaspo, M. L., Gabrieli, A. et al. (2013). Analysis of the DNA-binding profile and function of TALE homeoproteins reveals their specialization and specific interactions with Hox genes/proteins. *Cell Rep.* **3**, 1321-1333.
Prusky, G. T., Alam, N. M., Beekman, S. and Douglas, R. M. (2004). Rapid quantification of adult and developing mouse spatial vision using a virtual optomotor system. *Invest. Ophthalmol. Vis. Sci.* **45**, 4611-4616.
Puk, O., Dalke, C., Favor, J., de Angelis, M. H. and Graw, J. (2006). Variations of eye size parameters among different strains of mice. *Mamm. Genome* **17**, 851-857.
Puk, O., de Angelis, M. H. and Graw, J. (2013a). Lens density tracking in mice by Scheimpflug imaging. *Mamm. Genome* **24**, 295-302.
Puk, O., de Angelis, M. H. and Graw, J. (2013b). Longitudinal fundus and retinal studies with SD-OCT: a comparison of five mouse inbred strains. *Mamm. Genome* **24**, 198-205.
Ragge, N. K., Brown, A. G., Poloschek, C. M., Lorenz, B., Henderson, R. A., Clarke, M. P., Russell-Eggitt, I., Fielder, A., Gerrelli, D., Martinez-Barbera, J. P. et al. (2005). Heterozygous mutations of OTX2 cause severe ocular malformations. *Am. J. Hum. Genet.* **76**, 1008-1022.
Reis, L. M., Tyler, R. C., Schneider, A., Bardakjian, T., Stoler, J. M., Melancon, S. B. and Semina, E. V. (2010). FOXE3 plays a significant role in autosomal recessive microphthalmia. *Am. J. Med. Genet. A* **152A**, 582-590.
Reis, L. M., Tyler, R. C., Schilter, K. F., Abdul-Rahman, O., Innis, J. W., Kozel, B. A., Schneider, A. S., Bardakjian, T. M., Lose, E. J., Martin, D. M. et al. (2011). BMP4 loss-of-function mutations in developmental eye disorders including SHORT syndrome. *Hum. Genet.* **130**, 495-504.
Robinson, M. D., McCarthy, D. J. and Smyth, G. K. (2010). edgeR: a Bioconductor package for differential expression analysis of digital gene expression data. *Bioinformatics* **26**, 139-140.
Rosello-Diez, A., Arques, C. G., Delgado, I., Giovinazzo, G. and Torres, M. (2014). Diffusible signals and epigenetic timing cooperate in late proximo-distal limb patterning. *Development* **141**, 1534-1543.
Royo, J. L., Bessa, J., Hidalgo, C., Fernández-Miñán, A., Tena, J. J., Roncero, Y., Gómez-Skarmeta, J. L. and Casares, F. (2012). Identification and analysis of conserved cis-regulatory regions of the MEIS1 gene. *PLoS ONE* **7**, e33617.
Schimmenti, L. A., de la Cruz, J., Lewis, R. A., Karkera, J. D., Manligas, G. S., Roessler, E. and Muenke, M. (2003). Novel mutation in sonic hedgehog in non-syndromic colobomatous microphthalmia. *Am. J. Med. Genet. A* **116A**, 215-221.
Schulte, D. and Frank, D. (2014). TALE transcription factors during early development of the vertebrate brain and eye. *Dev. Dyn.* **243**, 99-116.
Schwarz, M., Cecconi, F., Bernier, G., Andrejewski, N., Kammandel, B., Wagner, M. and Gruss, P. (2000). Spatial specification of mammalian eye territories by reciprocal transcriptional repression of Pax2 and Pax6. *Development* **127**, 4325-4334.
Shen, Y., Yue, F., McCleary, D. F., Ye, Z., Edsall, L., Kuan, S., Wagner, U., Dixon, J., Lee, L., Lobanenkov, V. V. et al. (2012). A map of the cis-regulatory sequences in the mouse genome. *Nature* **488**, 116-120.
Sicinski, P., Donaher, J. L., Parker, S. B., Li, T., Fazeli, A., Gardner, H., Haslam, S. Z., Bronson, R. T., Elledge, S. J. and Weinberg, R. A. (1995). Cyclin D1 provides a link between development and oncogenesis in the retina and breast. *Cell* **82**, 621-630.
Slattery, M., Riley, T., Liu, P., Abe, N., Gomez-Alcala, P., Dror, I., Zhou, T., Rohs, R., Honig, B., Bussemaker, H. J. et al. (2011). Cofactor binding evokes latent differences in DNA binding specificity between Hox proteins. *Cell* **147**, 1270-1282.
Slavotinek, A. M. (2011). Eye development genes and known syndromes. *Mol. Genet. Metab.* **104**, 448-456.
Stankunas, K., Shang, C., Twu, K. Y., Kao, S.-C., Jenkins, N. A., Copeland, N. G., Sanyal, M., Selleri, L., Cleary, M. L. and Chang, C.-P. (2008). Pbx/Meis deficiencies demonstrate multigenetic origins of congenital heart disease. *Circ. Res.* **103**, 702-709.
Taranova, O. V., Magness, S. T., Fagan, B. M., Wu, Y., Surzenko, N., Hutton, S. R. and Pevny, L. H. (2006). SOX2 is a dose-dependent regulator of retinal neural progenitor competence. *Genes Dev.* **20**, 1187-1202.
The ENCODE Project Consortium (2012). An integrated encyclopedia of DNA elements in the human genome. *Nature* **489**, 57-74.
Voronina, V. A., Kozhemyakina, E. A., O'Kernick, C. M., Kahn, N. D., Wenger, S. L., Linberg, J. V., Schneider, A. S. and Mathers, P. H. (2004). Mutations in the human RAX homeobox gene in a patient with anophthalmia and sclerocornea. *Hum. Mol. Genet.* **13**, 315-322.
Waters, B. L., Allen, E. F., Gibson, P. C. and Johnston, T. (1993). Autopsy findings in a severely affected infant with a 2q terminal deletion. *Am. J. Med. Genet.* **47**, 1099-1103.
Weaver, R. G., Rao, N., Thomas, I. T. and Pettenati, M. J. (1991). De novo inv(2)(p21q31) associated with isolated bilateral microphthalmia and cataracts. *Am. J. Med. Genet.* **40**, 509-512.
White, T., Lu, T., Metlapally, R., Katowitz, J., Kherani, F., Wang, T. Y., Tran-Viet, K. N. and Young, T. L. (2008). Identification of STRA6 and SKI sequence variants in patients with anophthalmia/microphthalmia. *Mol. Vis.* **14**, 2458-2465.
Williamson, K. A. and FitzPatrick, D. R. (2014). The genetic architecture of microphthalmia, anophthalmia and coloboma. *Eur. J. Med. Genet.* **57**, 369-380.
Zhang, X., Friedman, A., Heaney, S., Purcell, P. and Maas, R. L. (2002). Meis homeoproteins directly regulate Pax6 during vertebrate lens morphogenesis. *Genes Dev.* **16**, 2097-2107.
Zhang, X., Rowan, S., Yue, Y., Heaney, S., Pan, Y., Brendolan, A., Selleri, L. and Maas, R. L. (2006). Pax6 is regulated by Meis and Pbx homeoproteins during pancreatic development. *Dev. Biol.* **300**, 748-757.

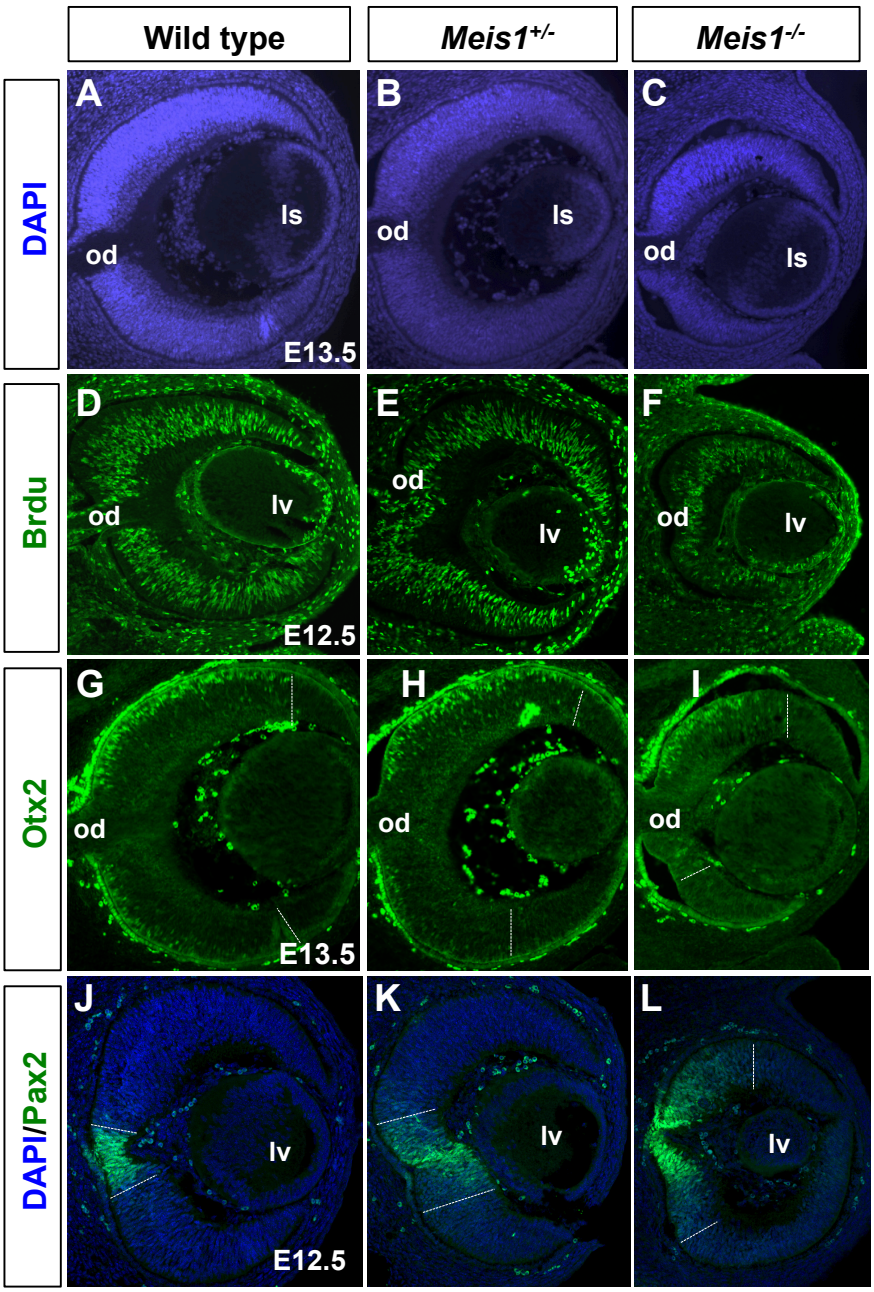

Supplementary Figure 1. Meis1 is cell autonomously required for retinal neurogenesis. A-I) Frontal cryostat sections through the optic cup of wt, *Meis1*$^{+/-}$ and *Meis1*$^{-/-}$ embryos at the stages indicated in the panels stained with DAPI to determine general optic cup morphology or immunostained with antibodies against BrdU, Otx2 and Pax2. Note the decrease in eye size and BrdU incorporation in the mutants. Neuronal differentiation, marked by Otx2 expression is also strongly decreased in both heterozygous and homozygous *Meis1* mutants. Similarly, the expression of Pax2, restricted to the optic disc in wt, in extended to both the dorsal and ventral retina in *Meis1*$^{-/-}$ embryos. This defect, although present, is less evident in *Meis1*$^{+/-}$ optic cup. Dotted lines in the different panels delineate the extent of marker labeling Abbreviations: lv, lens vesicle; od, optic disc.

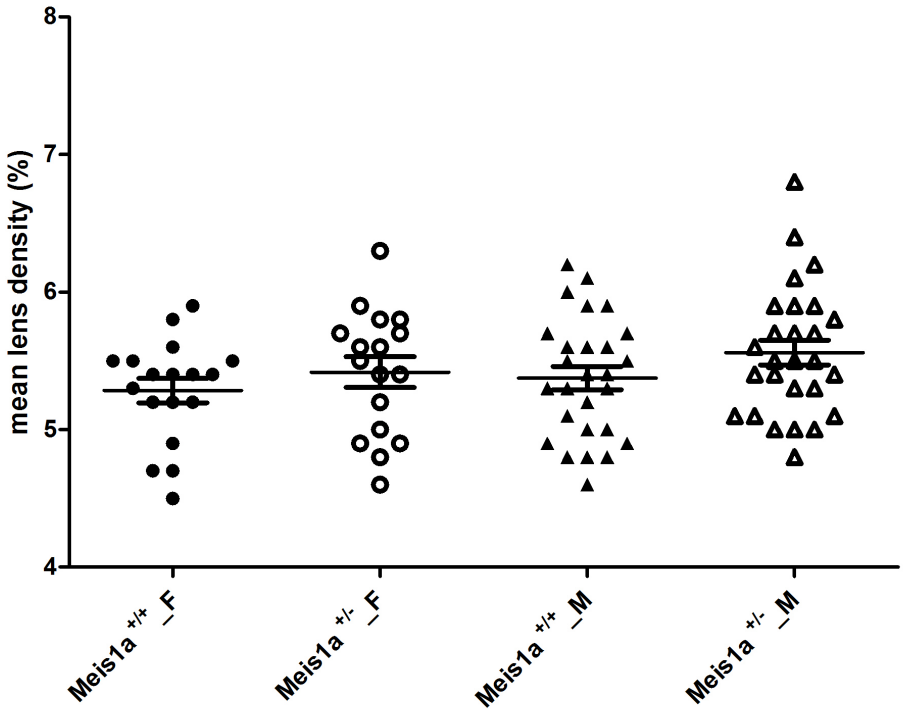

Supplementary Figure 2. Adult Meis+/- mice present no anterior segment abnormalities. The graph show the mean lens density, determined with a Pentacam, in male and female adult Meis+/- animals as compared to wt littermates. No differences were detected (mean ± S.E.M., scatter plot).

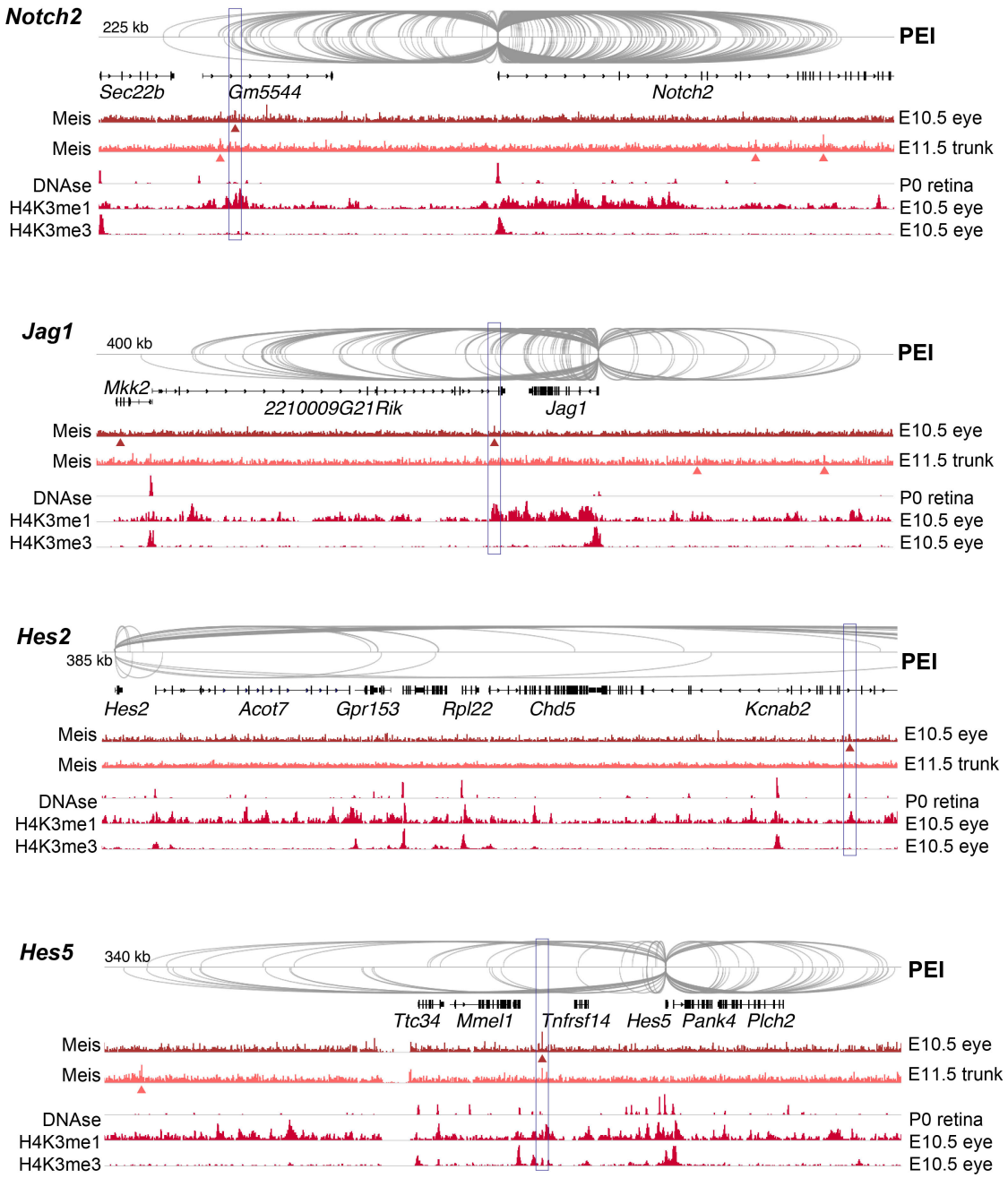

Supplementary Figure 3. Meis binding and histone modification profiles at Notch pathway genes. Representation of the *Notch2*, *Jag1*, *Hes2* and *Hes5* genes showing their described Promoter Enhancer Interactions (PEI) according to Shen et al. (Shen et al., 2012); the Meis1 ChIP seq read profile from E10.5 eye and E11.5 trunk (Penkov et al., 2013); the P0 DNAse-seq profile (from the ENCODE project; GEO:GSM1014188; (Consorum, 2012), and the H3K4me1 and H3K4me3 ChIP seq profiles. Detected Meis1 BS are shown by arrowheads below the read profiles. Boxes highlight the E10.5 eye Meis BS regions and their coincidence with Histone modifications and described enhancer promoter interactions.

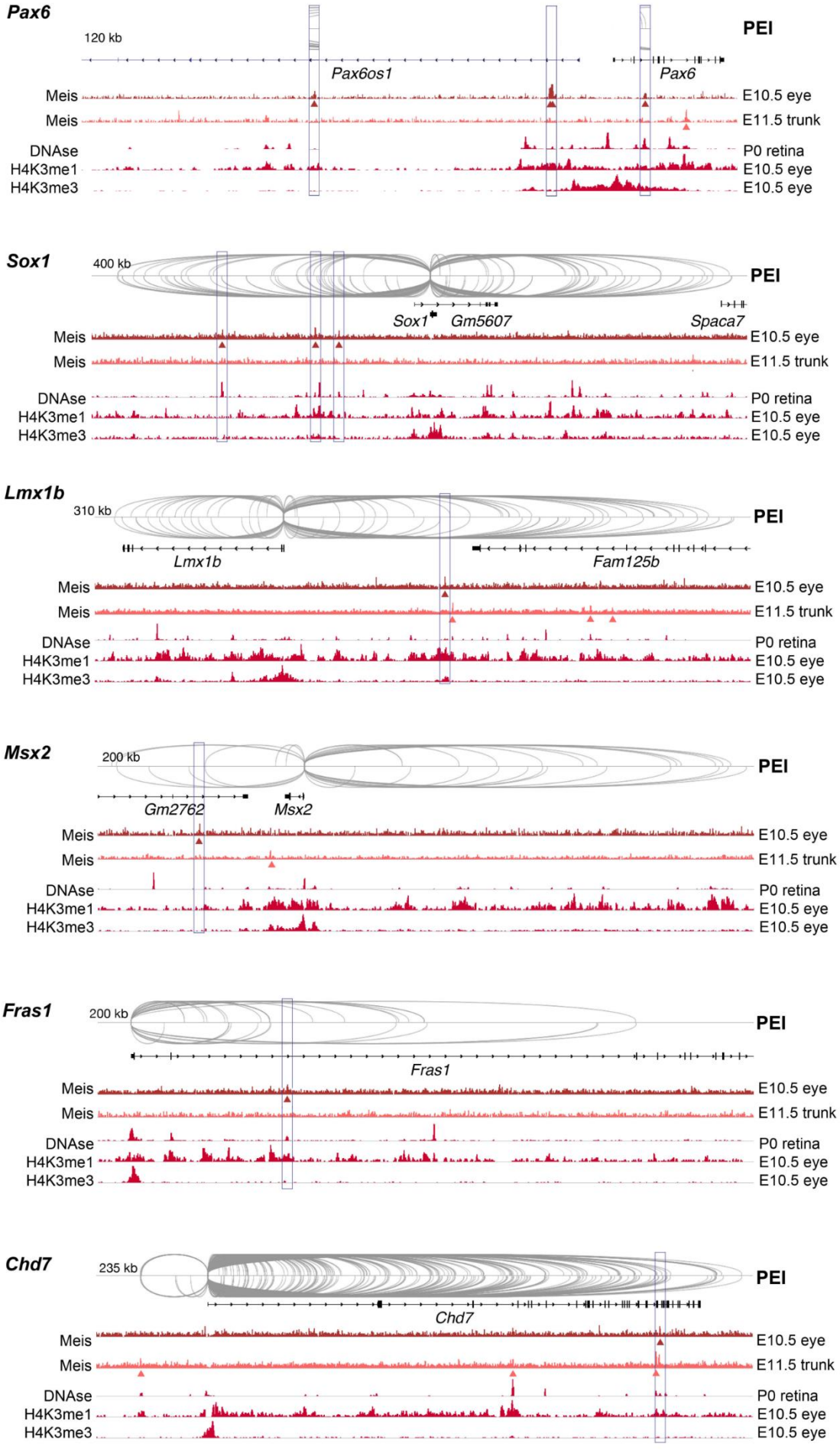
Pax6
120 kb
PEI
Pax6os1
Pax6
Meis
E10.5 eye
Meis
E11.5 trunk
DNAse
P0 retina
H4K3me1
E10.5 eye
H4K3me3
E10.5 eye
Sox1
400 kb
PEI
Sox1
Gm5607
Spaca7
Meis
E10.5 eye
Meis
E11.5 trunk
DNAse
P0 retina
H4K3me1
E10.5 eye
H4K3me3
E10.5 eye
Lmx1b
310 kb
PEI
Lmx1b
Fam125b
Meis
E10.5 eye
Meis
E11.5 trunk
DNAse
P0 retina
H4K3me1
E10.5 eye
H4K3me3
E10.5 eye
Msx2
200 kb
PEI
Gm2762
Msx2
Meis
E10.5 eye
Meis
E11.5 trunk
DNAse
P0 retina
H4K3me1
E10.5 eye
H4K3me3
E10.5 eye
Fras1
200 kb
PEI
Fras1
Meis
E10.5 eye
Meis
E11.5 trunk
DNAse
P0 retina
H4K3me1
E10.5 eye
H4K3me3
E10.5 eye
Chd7
235 kb
PEI
Chd7
Meis
E10.5 eye
Meis
E11.5 trunk
DNAse
P0 retina
H4K3me1
E10.5 eye
H4K3me3
E10.5 eye

Supplementary Figure 4. Meis binding and histone modification profiles at microphthalmia-related genes. Representaon of the *Pax6*, *Sox1*, *Lmx1b, Msx2, Fras1* and *Chd7* genes showing their described Promoter-Enhancer Interacons (PEI) according to (Shen et al., 2012); the Meis1 ChIP-seq read profile from E10.5 eye and E11.5 trunk (Penkov et al., 2013); the P0 DNAse-seq profile (from the ENCODE project; GEO:GSM1014188), and the H3K4me1 and H3K4me3 ChIP-seq profiles. Detected Meis1-BSs are shown by arrowheads below the read profiles. Boxes highlight the E10.5 eye Meis-BS regions and their coincidence with Histone modification marks and described enhancer-promoter interactions.

Table S1. Genes upregulated in *Meis1* knockout

Click here to Download Table S1

Table S2. Genes downregulated in *Meis1* knockout

Click here to Download Table S2